Mifsud, K. R., & Reul, J. M. H. M. (2016). Acute stress enhances heterodimerization and binding of corticosteroid receptors at glucocorticoid target genes in the hippocampus. *Proceedings of the National Academy of Sciences of the United States of America*, *113*(40), 11336-11341. https://doi.org/10.1073/pnas.1605246113

PNAS 2016-05246RR

Acute stress enhances heterodimerization and binding of corticosteroid receptors at glucocorticoid target genes in the hippocampus

Karen R. Mifsud & Johannes M.H.M. Reul*

Neuro-Epigenetics Research Group, University of Bristol, Dorothy Hodgkin Building, Whitson Street, Bristol BS1 3NY, UK

***Correspondence:**

Professor Johannes M.H.M. Reul

Neuro-Epigenetics Research Group

University of Bristol

Dorothy Hodgkin Building

Whitson Street

Bristol BS1 3NY, UK

Hans.Reul@bristol.ac.uk

Major classification: Biological Sciences

Minor classification: Neuroscience

Short title: Stress-induced MR and GR GRE-binding

Key words: Stress, Mineralocorticoid Receptor, Glucocorticoid receptor, Heterodimerization, Hippocampus, Gene Transcription, Epigenetics

Abstract

A stressful event results in secretion of glucocorticoid hormones (GCs), which bind to mineralocorticoid (MRs) and glucocorticoid receptors (GRs) in the hippocampus to regulate cognitive and affective responses to the challenge. MRs are already highly occupied by low GC levels under baseline conditions, whereas GRs only become substantially occupied by stress- or circadian-driven GC levels. Currently, however, the binding of MRs and GRs to GC responsive elements (GREs) within hippocampal GC target genes under such physiological conditions *in vivo* is unknown. We found that forced swim (FS) stress evoked increased hippocampal RNA expression levels of the GC-responsive genes *Fkbp5*, *Per1* and *Sgk1*. Chromatin immuno-precipitation (ChIP) analysis showed that this stressor caused substantial gene-dependent increases in GR binding and, surprisingly, also in MR binding to GREs within these genes. Different acute challenges, including novelty, restraint and FS stress, produced distinct GC responses but resulted in largely similar MR and GR binding to GREs. Sequential and Tandem ChIP analyses showed that after FS stress MRs and GRs bind concomitantly to the same GRE sites within *Fkbp5* and *Per1*, but not *Sgk1*. Thus, after stress MRs and GRs appear to bind to GREs as homo- and/or heterodimers in a gene-dependent manner. MR binding to GREs at baseline appears to be restricted, whilst after stress GR binding may facilitate co-binding of MR. This study reveals that the interaction of MRs and GRs with GREs within the genome constitutes an additional level of complexity in hippocampal GC action beyond expectancies based on ligand-receptor interactions.

Significance Statement

Glucocorticoid hormones (GCs) are important mediators of the stress response and are implicated in the etiology of stress-related psychiatric disorders. GCs act via mineralocorticoid (MRs) and glucocorticoid receptors (GRs) in the hippocampus resulting in altered transcription of target genes. Currently, however, little information is available about how they interact with the genome after stress *in vivo*. Here we demonstrate that an acute stressful challenge results in an increased interaction of both MRs and GRs with their genomic recognition sites. Moreover, they may interact with these sites not just as homodimers but also as heterodimers, the extent of which is highly gene-dependent. These findings provide insight into how MRs and GRs interact with the hippocampal genome after stress *in vivo*.

\body

Introduction

Adrenal glucocorticoid (GC) hormones play a pivotal role in orchestrating adaptive responses to stressful challenges to maintain health and wellbeing. Acute surges in GC secretion after stress are beneficial for the organism whereas aberrant secretion, as a result of chronic stress or traumatic experiences, is damaging and increases susceptibility to mental disorders such as major depression, anxiety and posttraumatic stress disorder (PTSD).

Over 40 years ago, McEwen et al. (1) discovered that GCs act through receptors located in the brain, primarily the hippocampus. In 1985, Reul and de Kloet (2) reported that these steroid hormones bind to two distinct types of receptors, the mineralocorticoid (MR) and the GC receptor (GR), in this limbic brain region where these receptors are co-localized in neurons (2, 3). Due to the extraordinary difference in binding affinity of MRs (K_d 0.1-0.5 nM for binding corticosterone (CORT), the endogenous GC of rats and mice) and GRs (K_d 2-5 nM) there were marked differences in receptor occupancy between these receptors under baseline and stress conditions (2, 4). MRs are already >80% occupied with endogenous GCs under early morning (AM) baseline conditions whereas GRs only become substantially occupied by elevated GC levels, such as after stress and at the circadian peak of GC secretion. These data gave rise to the concept that MRs exert tonic actions on brain whereas GRs mediate the negative feedback and long-term cognitive changes evoked by GCs (2, 4, 5).

MR and GR are mainly intracellular receptors that act as ligand-dependent transcription factors. After binding of GCs the receptors are translocated to the nucleus, with the help of co-chaperones, and bind to specific GC response elements (GREs) within the DNA of GC-inducible genes to elicit transcriptional responses (6, 7). The molecular mechanisms underpinning the interaction of MRs and GRs with the genome have been primarily studied *in vitro*, predominantly using chromatin immuno-precipitation (ChIP), allowing the investigation of transcription factor binding to recognition sites within the genome. ChIP has been used to study the interaction of GR with GREs in GC target genes in cell cultures *in vitro* and in pharmacological studies *in vivo* (8, 9). Until now, however, the binding of MR and GR to GREs within GR target genes under

physiological conditions in hippocampus tissue *in vivo* has never been studied. Thus, currently it is unknown how stressful challenges impact on MR and GR binding to GREs within the genome *in vivo*.

A long-standing question is whether, in addition to forming MR/MR and GR/GR homodimers, MRs and GRs also form MR/GR heterodimers and interact as such at the genomic level. In fact, the concept of heterodimer formation by these steroid receptors and their ability to bind DNA is based on studies *in vitro* and has not been shown *in vivo*. Work using cell cultures and cell-free approaches indicate that MR/GR heterodimers may form under conditions *in vitro* (10-12). In addition, Trapp et al. found stronger DNA binding and gene transcriptional effects *in vitro* under conditions that favored MR/GR heterodimerization (10). Neither study investigated MR/GR heterodimer binding to GREs within the genome. Moreover, evidence that MR/GR heterodimerization and DNA binding is taking place under physiological conditions *in vivo* is presently lacking.

We investigated the interaction of MRs and GRs with GREs within the well-known GC target genes *Fkbp5* (FK506-binding immunophilin 51), *Per1* (Period 1) and *Sgk1* (serum- and GC-inducible kinase 1). These genes are involved in GR ligand binding affinity (13), circadian neuronal activity (14), and neuronal plasticity processes (15), respectively, and were transcriptionally activated after FS stress. Using ChIP, we found that after stress MRs and GRs bound transiently to GRE sites within these GC target genes, albeit in a gene-dependent manner. For MR the significant increase in DNA binding after stress was surprising given the high GC occupancy of this receptor under baseline AM conditions challenging the notion that high receptor occupancy would correlate with high DNA binding. Furthermore, as revealed by Tandem ChIP, MRs and GRs bind concomitantly to the same GRE sites within *Fkbp5* and *Per1* but not *Sgk1* after stress, indicating that these steroid receptors, in addition to forming homodimers, indeed appear to bind to GREs as heterodimers. Thus, our study shows that, after stress, MRs and GRs may access the genome as homo- and/or heterodimers and in a gene-dependent manner.

Results

Acute stress increases transcription of GC target genes across all hippocampal subregions

A single 15 min FS challenge resulted in a significant, time-dependent, increase in the transcription of the classic GC-dependent genes *Fkbp5* (Fig. 1A), *Per1* (Fig. 1C) and *Sgk1* (Fig. 1E) in the dentate gyrus. Very similar patterns of transcriptional activation were found in the CA regions (Fig. 1B, D, F) and ventral hippocampus (Fig. S1). The time course of stress-induced gene transcription, and the conversion time for splicing heteronuclear RNA (hnRNA) to mRNA, was gene-specific with *Fkbp5* peaking at 60 min (hnRNA) and significant increases in mRNA expression by 180 min whilst RNAs of *Per1* and *Sgk1* peaked earlier (hnRNA, 30 min; mRNA, 60 min). The peaks in *Per1* and *Sgk1* hnRNA corresponded with the peak in plasma CORT after FS (30 min; Fig. S2), but the *Fkbp5* hnRNA response was clearly delayed. As the RNA responses were highly similar between the hippocampal sub-regions, we performed subsequent ChIP analyses on whole hippocampus tissues.

FS transiently increases MR and GR binding to GREs within hippocampal GC target genes

Presently, it is unknown whether stress-induced transcriptional activation of GC-dependent genes involves physical interaction of MRs and GRs with GREs within these genes. Using ChIP, we studied MR and GR binding to GREs within *Fkbp5* (GRE2), *Per1* and *Sgk1* (see Fig. S3 for within gene location of targeted GREs) in hippocampal chromatin from rats killed under early morning baseline conditions (AM), at various time points after FS stress, or under late afternoon baseline conditions (PM; Fig. 2). FS stress resulted in a highly significant, transient increase in corticosteroid receptor binding to all GC target genes investigated (Fig. 2) that largely paralleled the changes in plasma CORT levels (Fig. S2). The peak in MR and GR binding (at 30min) coincided with (*Per1*, *Sgk1*) or preceded (*Fkbp5*) the increases in hnRNA levels after stress (Fig. 1). In contrast to GR (Fig. 2B, D, F), MR binding to GREs was already near-maximal at 15min (Fig. 2A, C, E). After stress, MR binding to GREs increased gene dependently between 1.5- (*Sgk1*) and 6-fold (*Fkbp5*) (Fig. 2), which was surprising given that MR occupancy by endogenous GCs is already very high (>80%) under baseline AM conditions (2, 4). Thus, in case of MR, high receptor occupancy does not predict or guarantee high GRE binding. Occupancy of GRs by endogenous GCs after stress was shown to follow the course of the

plasma GC concentration (2, 4). Fig. 2B, D and F show that the binding of GRs to the different GREs was highly responsive to stress and followed the pattern of plasma GC levels (Fig. S2) and GR occupancy levels (2, 4). The magnitude of the stress-evoked enhancement in binding of MR and GR to GREs was highly gene-dependent with highest increments found in *Fkbp5* GRE2 and in *Per1* GRE, and smaller increases in *Sgk1* GRE. This indicates that, under both baseline and stress conditions, accessibility of GRE sites within GC target genes appears to be different within hippocampal cells. Comparison of MR and GR binding between baseline AM and PM presents a clear circadian variation in the interaction of both receptors with the target gene GREs, except for MR binding to the *Sgk1* GRE, which failed to reach statistical significance (Fig. 2). These observations show that rises in MR and GR binding can occur in response to circadian-driven increases in circulating GCs (Fig. S2), independent of stress.

Comparison of different stressors regarding MR and GR binding to GC target genes

Subsequently, we investigated whether the degree of MR and GR binding to GREs depends on the severity of the stressor. The plasma CORT levels after novelty (NE), restraint (RS) and FS stress were ~230, 670 and 1160 ng/ml, respectively ((16); Fig. S2; baseline AM levels: ~10 ng/ml). All stressors caused substantial increases in MR and GR binding to all target gene GREs investigated (Fig. 3). Overall, the magnitude of the binding responses was gene-dependent, with *Fkbp5* (GRE2) and *Per1* showing much higher responses than *Sgk1*. Remarkably, however, although these stressors are well known to produce distinct GC responses, binding of MRs and GRs to a GRE within a particular gene was very similar. For instance, NE and FS stress evoke very different plasma GC levels, nevertheless, binding of MRs and GRs to GREs was not different between these stressors (Fig. 3). RS, generating lower plasma GC responses than FS, resulted in significantly higher GR binding to *Fkbp5* GRE2 and *Per1* GRE (Fig. 3B). Thus, MR and GR binding to GREs after stress is virtually an on/off switch possibly controlled by other factors in addition to GCs.

Selective MR and GR binding to GREs within intron 5 of the *Fkbp5* gene

GR regulation of the *Fkbp5* gene occurs predominantly via interaction with intronic GREs (17). Previously, a study *in vitro* has shown that the intron-5 GRE2 site (Fig. S3) is crucial for GC stimulation of *Fkbp5* gene

transcription whereas the GRE1 site within this intron was inactive (17). In Figs. 2 and 3, we presented significant increases in MR and GR binding to the *Fkbp5* GRE2 site after FS. In Fig. S4, we compared receptor binding to *Fkbp5* GRE1 and GRE2 at AM and 30min after FS. In contrast to GRE2, there was no significant increase in MR or GR binding to GRE1 after FS, which corresponds with reports (17) that this site is not actively involved in transducing GC effects on *Fkbp5* transcription.

MR and GR interaction at GREs within GC target genes

Our results show that both MRs and GRs bind to GREs within target genes after stress and at the circadian peak of GC secretion. It is unclear however whether the receptors bind to separate GREs, thus strictly as homodimers, or whether they can bind concomitantly at the same GRE site, as heterodimers. Although there are indications from cell culture and cell-free studies (10-12) that MRs and GRs may interact with GREs as heterodimers, direct evidence that this may be occurring at the chromatin level under physiological conditions *in vivo* is lacking. To resolve this question we adopted a serial ChIP approach. We reasoned that if MR and GR interact at the same GREs within a given gene, then IP of one receptor would lead to relative depletion of the other receptor. Fig. 4 shows that if ChIP was conducted after FS stress for either receptor first, followed by a second ChIP for the other receptor on the Unbound fraction, then significantly less binding for this receptor at *Fkbp5* GRE2 was measured after the second ChIP. This result indicates that ChIP for MR leads to a reduced ChIP outcome for GR and vice versa, providing indirect evidence that MRs and GRs are binding concomitantly to the same GREs. This was only observed after FS but not in the AM and PM samples. A similar result was found regarding GR binding to the *Per1* and *Sgk1* GREs conducted after MR ChIPs (Fig. S5B, D), but not for MR binding to these GREs after GR ChIP (Fig. S5A, C), possibly because the stress-induced increases in MR binding to the *Per1* and *Sgk1* GREs are lower in magnitude than the rise in binding to the *Fkbp5* GRE2 (Fig. 2). This experiment provides indirect evidence that MR and GR may interact in part at the same GRE sites within GC target genes after stress.

Evidence supporting MR-GR heterodimerization at GREs within GC target genes

To provide direct evidence for concomitant binding of MR and GR to the same GRE sites within GC target genes, we applied a Tandem ChIP protocol. We conducted an MR ChIP or a GR ChIP on hippocampal chromatin of AM or FS (30min) rats and, subsequently, we re-ChIPed the eluted IP'd chromatin with an antibody against the same (ChIP and re-ChIP samples: MR→MR, GR→GR) or the other receptor (MR→GR, GR→MR). This was followed by qPCR analysis of GREs within *Fkbp5* (GRE2; Fig. 5), *Per1* and *Sgk1* (Fig. S6). Based on the different Tandem ChIP combinations, the MR→GR and GR→MR Tandem ChIP selectively revealed concomitantly bound MR and GR (indicating MR/GR heterodimer formation) at the qPCR-targeted GRE. The MR→MR and the GR→GR combinations determine the binding of the respective homodimers (MR/MR and GR/GR, respectively) plus the binding of MR/GR heterodimers. Accordingly, the difference between the MR→MR or the GR→GR combination and the parallel MR→GR or GR→MR combinations would provide an estimate for the contribution of the respective MR/MR and GR/GR homodimers to the ChIP result. These Tandem ChIPs provide tangible but not absolute evidence for MR/GR heterodimerization as MR and GR co-occupancy of GREs could possibly be occurring in conjunction with other proteins.

Our results show that the extent of putative homodimer and heterodimer formation at GREs under AM and stress conditions was highly gene dependent (Fig. 5, S6). Regarding *Fkbp5* GRE2, under AM conditions, it appeared that there was higher MR/MR homodimer binding than MR/GR or GR/GR binding but differences were not statistically significant (Fig. 5). FS resulted in a significant increase in the binding of putative MR/GR heterodimers to *Fkbp5* GRE2 as revealed by both MR→GR and GR→MR Tandem ChIPs (Fig. 5A, B). As there was no significant difference between the MR→MR and the MR→GR results, it is likely that MRs participate in binding to this GRE only together with GRs as heterodimers, and not as MR/MR homodimers (Fig. 5A). After stress, the substantial difference between the GR→GR and the GR→MR results (Fig. 5B) indicates that, in addition to forming heterodimers with MRs, GRs also bound significantly as GR/GR homodimers.

Under baseline conditions and after FS stress, the MR→GR ChIP result was significantly lower than the MR→MR result at *Per1* GRE, indicating that, under these conditions, corticosteroid receptors may be binding as both MR/MR homodimers and MR/GR heterodimers (Fig. S6A). In addition, the rise in GR→GR binding after stress at *Per1* GRE was highly significant, but the increase in GR→MR binding failed to reach

statistical significance (Fig. S6B). In conjunction, these Tandem ChIP data suggest that after stress MRs and GRs bind to the *Per1* GRE largely as GR/GR homodimers and to a lesser extent as MR/MR homodimers and MR/GR heterodimers (Fig. S6A, B). At the *Sgk1* GRE, forced swimming increased both MR→MR and GR→GR binding (Fig. S6C, D). Given that FS-induced binding in MR→GR and GR→MR failed to reach statistical significance it is likely this gene is regulated predominantly by homodimers (Fig. S6C, D).

Discussion

This study shows that in the hippocampus an acute stressful challenge transiently increases MR and GR binding to GREs within the GC target genes *Fkbp5*, *Per1* and *Sgk1* and enhances transcription of these genes. Surprisingly, despite the high occupancy level of MRs under baseline conditions (2, 4), a relatively low binding of this receptor to GREs was observed under these conditions. Different stressors, although evoking different GC peak levels, resulted in largely similar increases in MR and GR binding to GREs within these genes. Overall we observed that the interaction of MRs and GRs with GREs under the various conditions investigated was highly gene dependent. Sequential and Tandem ChIP analyses showed that after stress MRs and GRs may bind as homodimers as well as heterodimers to *Fkbp5* and *Per1* GREs whereas *Sgk1* GRE appeared only to be bound by the respective homodimers. These data show that the interaction of GRs with the genome appears to be a reflection of circulating GC levels and expected receptor occupancy levels whereas MRs' genomic interaction may be restricted under baseline AM conditions and/or depend on co-binding with GRs. Together, these results reveal gene-dependent and receptor-specific modes of interactions with the genome, which cannot be predicted solely on the basis of hormone concentrations and receptor occupancy levels.

FS caused a significant increase in RNA expression of *Fkbp5*, *Per1* and *Sgk1*, which is consistent with their well-known responsiveness to GCs (17-20). The hnRNA levels for *Per1* and *Sgk1* peaked at 30 min whereas *Fkbp5* hnRNA levels reached their maximal levels later, at 60 min. The mRNA expression levels after stress followed the hnRNA responses with a delay of at least 30 min in all genes, indicative of time required for the splicing process. Whereas GREs in the *Per1* and *Sgk1* genes are located in their proximal promoter

region, in the *Fkbp5* gene the transcriptionally active GREs are located within intronic sequences (6, 17-19, 21, 22). In the rat, GRE2 within intron 5 has been identified as being particularly important for GC-induced *Fkbp5* transcription (17). Receptor-bound GREs within introns of the *Fkbp5* gene are thought to stimulate gene transcription through chromatin remodelling including loop formation that allows the direct interaction of the intronic region with the transcriptional start site (TSS; (23, 24)). Such a process is anticipated to require more time than the direct transactivational stimulation originating from promoter-located GREs like in *Per1* and *Sgk1*, which may explain the differences in the time course of the stress-induced hnRNA (and mRNA) responses despite similar time courses of MR and GR binding to these GREs.

Although corticosteroid receptor interaction with GC target genes has been studied under pharmacological conditions (e.g. GC injections in ADX rats; (9)), the interaction of MRs and GRs with such genes in the hippocampus under GC-relevant physiological conditions has not been studied to date. Under baseline conditions, MR and GR binding levels at GREs were relatively low in the early morning but rose significantly during the day reaching significantly elevated levels late afternoon, except for MR binding at the *Sgk1* GRE. An acute FS challenge evoked a substantial rise in receptor binding to GREs with MRs reaching near-maximal level at 15 min and GR binding peaking at 30 min. These peak binding levels superseded the respective levels observed at baseline PM. The receptor binding profiles at baseline and after stress largely followed the circulating CORT levels. Regarding GR binding to GREs this may have been expected given that studies had shown GR occupancy by endogenous GCs critically depends on circulating hormone concentrations (2, 4). The peak in GR binding at 30 min after stress concurs with the peak in stress-induced plasma GC levels but, in view of recent findings on stress-induced free CORT levels (16), this was unexpected. Recent microdialysis studies *in vivo* have shown that after FS stress the peak in free CORT in the hippocampus is delayed 20-30 min compared with the plasma hormone response (16, 25). Thus, as the free CORT concentration is the critical parameter for hormone-receptor interaction, maximal GR binding to GREs after stress would be expected to occur at 60 min, rather than at 30 min. At 60 min post-stress, however, GR (and MR) binding levels were substantially lower than at 30 min. Thus, GR's interaction with

GREs (and MR's as well) is only partly determined by GC levels indicating the on and off status regarding GREs is actively regulated by additional molecular factors (26).

The binding profile of MRs to GREs under baseline and stress conditions is remarkable because Reul and de Kloet reported 30 years ago that hippocampal MRs are at least 80% occupied with endogenous GCs under all physiological conditions studied (2, 4) and occupancy levels only dropped after adrenalectomy (4). Therefore, we had expected that MR binding to GREs to be relatively high under baseline AM conditions with only small increases after stress. Our results however show a different picture: relatively low binding at baseline AM and substantial increases after stress and at baseline PM (except *Sgk1* GRE). Thus, high occupancy of MR does not translate into high binding to GREs. One reason may be that under baseline AM conditions MR binding to GREs is restricted due to an action of a steroid receptor co-repressor like DAXX (death associated protein), which after stress is expunged and/or exchanged for a steroid receptor co-activator like FAF-1 (Fas-associated factor 1). DAXX and FAF-1 are hippocampal proteins that have been shown to modulate MR transcriptional activity in hippocampal cells *in vitro* (27). Alternatively, MR binding to GREs may be weak as supported by early transfection studies *in vitro* (28). Trapp et al (10) showed that DNA binding of MR was low in COS cells solely transfected with MR (cf. GR) but could be increased dramatically when both receptors were transfected together. Furthermore, transcriptional activity of co-transfected receptors was higher than that of separately transfected receptors (10). Thus, MR binding in the absence of activated GRs, as is the case under baseline AM conditions, is weak, which changes considerably once GRs become activated due to stress-induced GC production. In other words, MRs appear to require GRs for substantial binding to GREs to occur. This notion is consistent with MRs and GRs heterodimerizing after stress.

In absolute terms, MR and GR binding to GREs within *Fkbp5* and *Per1* after stress was overall substantially higher than receptor binding observed to *Sgk1* GRE. As results are from the same ChIP DNA samples, these binding profiles are directly comparable. The observed differences in receptor binding were consistent across the different stressors. As each hippocampal cell contains two copies of each gene (if located on

autosomal chromosomes), theoretically, MR and GR binding to GREs could be similar but this is clearly not the case. Possibly, there is a less availability of the *Sgk1* GRE for binding compared with the *FKbp5* GRE2 and *Per1* GRE because, in a significant number of hippocampal cells, the gene may be located within inactive, condensed chromatin. In situ hybridization analysis suggests that *Sgk1* mRNA is indeed primarily expressed in hippocampal pyramidal neurons whereas *Fkbp5* and *Per1* mRNA is ubiquitously expressed in hippocampal neurons (29). Alternatively, there may be differences at the GRE level in terms of its nucleotide sequence as well as involvement of local modulators (e.g. steroid receptor co-regulators) affecting the affinity and stability of receptor-GRE interactions. Our work points to a role of other molecular mechanisms *in vivo* in addition to GRE nucleotide sequence as although both GRE1 and GRE2 within the *Fkbp5* present ideal nucleotide consensus sequences, MR and GR binding to these GREs is dramatically different. Whereas GRE2 shows significant increases in MR and GR binding after FS, GRE1 shows no significant change in binding. Our findings correspond with transcriptional analyses *in vitro* showing that GRE2 is a transactivationally active site whereas GRE1 is not (17) and may be explained by distinct accessibility of GRE1 versus GRE2 as a result of epigenetic and other molecular (e.g. steroid receptor co-regulators) mechanisms (23, 24, 26). These observations are consistent with our notion that MR and GR binding to GREs within the genome is highly controlled at the cellular level as well as the single gene level.

To investigate stressor specificity and the role of different levels of stress-induced GC levels we compared the effects of FS with those of NE and RS. FS and RS are strong stressors resulting in high GC responses whereas NE is regarded as a mild psychological stressor leading to moderate increases in plasma hormone levels (16). MR binding to GREs was very similar after the different stressors albeit with consistent inter-gene differences. Apparently, the mechanisms triggering MR binding to GREs are independent of the extent of stress-induced GC responses and other stressor-specific mediators. The independence of GC responses is not surprising as MRs are already highly occupied at baseline AM GC levels (2, 4). Our findings regarding GR binding to GREs were however surprising because despite the substantial difference in GC responses between stressors, the interactions of GRs with GREs were largely similar. These observations underscore that the GC response is not an all-determining factor in the genomic action of GRs (and MRs). It appears

that additional, stressor-specific factors are involved in determining GR binding to GREs in hippocampal cells including signalling pathways, epigenetic factors and local modulators. An additional factor may be the duration of the stressful experience: the RS (and NE) experience lasted the full 30 min until death whereas FS lasted 15 min after which the rats were returned to their home cages for the remaining 15 min. Therefore, the shorter lasting FS challenge may have allowed rats to shut down the stress response resulting in lower GR binding levels. Elucidation of the factors determining GR (and MR) interaction with the genome should be an intriguing challenge for future research.

To study if MR and GR are acting separately (as homodimers) to stimulate transcription of GC target genes, or possibly together in a complex, we initially performed a serial ChIP, first with one antibody (anti-MR or anti-GR) and then re-ChIPed the Unbound fraction using the opposite receptor antibody (either MR or GR). The rationale was that if GR and MR were interacting at the same GRE, IP of one DNA-bound receptor with the first antibody would also result in IP of the other receptor into the Bound fraction and deplete it from the Unbound fraction. A subsequent ChIP for the 'other' receptor on the Unbound fraction from the first ChIP would recover less target DNA compared with the amount recovered in the original ChIP. If, however, MR and GR were not bound to the same DNA strand, but instead bound to the same GRE location but on different strands, recovered DNA (covering this GRE site) would be comparable between ChIPs performed on both the original chromatin and the Unbound fraction of opposite receptor ChIP. We found that MR binding to GREs after stress was substantially reduced if GRs had been removed from the sample by IP previously, and vice versa. These effects were most clear for the *Fkbp5* GRE2, most likely because this GRE presented the largest stress-induced MR binding response. Cross-receptor depletion was only observed in hippocampal chromatin samples from stressed rats, but not from baseline PM animals, ruling out that depletion is the result of an assay artefact and indicating that MRs and GRs interact concomitantly with GREs within GC target genes specifically after stress. We used a more direct approach to investigate MR and GR interaction at GREs *in vivo* utilizing MR→GR and GR→MR Tandem ChIPs, which only IP GRE DNA bound to both MR and GR at the same time. The results show that after stress MRs and GRs bind concomitantly to the same GRE sites within *Fkbp5* and *Per1* genes, possibly through the formation of

heterodimers. Previous Co-IP experiments in a cell-free system have shown that MRs and GRs can heterodimerize in solution (11); our work provides evidence to support that this can occur at the DNA template *in vivo*. Moreover, after stress MRs and GRs may bind to GREs as heterodimers as well as homodimers but with striking gene-dependent differences. After stress, there appeared to be a strong recruitment of MR/GR heterodimers at the *Fkbp5* GRE2, less so at the *Per1* GRE, and very low recruitment at the *Sgk1* GRE. Thus, local chromatin status possibly defined by epigenetic factors in conjunction with co-regulatory factors may determine the level of recruitment as well as preference for homo- versus heterodimer binding. MR and GR co-transfection studies indicated that formation of the MR/GR heterodimer results in stronger GRE binding and greater reporter gene responses than shown by the respective homodimers (10). Presently, the gene transcriptional significance of MR/GR heterodimer formation is unclear. Our findings allow the study of the significance of heterodimer formation for gene transcriptional responses using pharmacological approaches as well as high-throughput sequencing methods.

Based on receptor occupancy studies, 30 years ago de Kloet and Reul proposed a concept on the role of MRs and GRs in the effects of GCs on the brain (2, 5). In view of its constant high occupancy it was thought that MRs exert a tonic influence on hippocampus function, including neuronal excitability, HPA axis activity, sympathetic outflow, and cognitive behaviour (2, 5, 30). GRs only became significantly occupied by elevated GC levels and were thought to exert negative feedback action on HPA axis activity and facilitate memory formation of stressful events (2, 5, 31). In view of our present data, this concept may require adjustments. The interaction of MRs and GRs with GREs under baseline and stress conditions and its gene transcriptional consequences appear much more complex than originally thought. The terminology tonic and feedback falls short in view of the multitude of mechanisms controlling the interaction of these steroid receptors with GRE sites including the highly diverse molecular processes governing accessibility of such sites within different genes and different cells and, moreover, their distinct, gene-specific way to interact with GREs probably as homodimers and heterodimers. This complexity may further grow after MR and GR binding has been conducted across the entire genome by ChIP-Sequencing. The present work has laid the basis to

continue elucidating the critical question of how GCs affect brain function. The answer to this question may hold the key to resolving stress-related disorders.

Materials and Methods

Animals and Stress Procedures: Male Wistar rats (150-175 g) were purchased from Harlan and group housed. Rats were forced to swim for 15 min in 25 °C water, subjected to RS or NS, or left undisturbed (32). Rats were killed under baseline conditions or at the indicated times after stress (see figure legends). **Tissue Preparation:** After decapitation, the entire hippocampus was dissected or the dentate gyrus and CA regions were micro-dissected from the dorsal hippocampus. Tissues were snap frozen in liquid N2 and stored at -80 °C. **ChIP, RNA Analysis, and qPCR:** ChIP and RNA extraction were performed using published methods (33). **Statistical Analysis:** Data were analyzed by ANOVA and appropriate post hoc tests. For more information on Materials and Methods, see SI Materials and Methods.

Acknowledgments

The authors thank Dr S.D. Carter for her help and reading the manuscript and BBSRC for grant support (Grant Ref.: BB/K007408/1).

References

1. McEwen BS, Weiss JM, & Schwartz LS (1968) Selective retention of corticosterone by limbic structures in rat brain. *Nature* 220(5170):911-912.
2. Reul JMHM & de Kloet ER (1985) Two receptor systems for corticosterone in rat brain: microdistribution and differential occupation. *Endocrinology* 117(6):2505-2511.
3. Reul JMHM & de Kloet ER (1986) Anatomical resolution of two types of corticosterone receptor sites in rat brain with in vitro autoradiography and computerized image analysis. *J Steroid Biochem* 24(1):269-272.
4. Reul JMHM, van den Bosch FR, & de Kloet ER (1987) Relative occupation of type-I and type-II corticosteroid receptors in rat brain following stress and dexamethasone treatment: functional implications. *J Endocrinol* 115(3):459-467.
5. De Kloet ER & Reul JMHM (1987) Feedback action and tonic influence of corticosteroids on brain function: a concept arising from the heterogeneity of brain receptor systems. *Psychoneuroendocrinology* 12(2):83-105.
6. Evans RM (1988) The steroid and thyroid hormone receptor superfamily. *Science* 240(4854):889-895.
7. Beato M (1989) Gene regulation by steroid hormones. *Cell* 56(3):335-344.
8. Datson NA*, et al.* (2011) Specific regulatory motifs predict glucocorticoid responsiveness of hippocampal gene expression. *Endocrinology* 152(10):3749-3757.

9. Polman JA, de Kloet ER, & Datson NA (2013) Two populations of glucocorticoid receptor-binding sites in the male rat hippocampal genome. *Endocrinology* 154(5):1832-1844.
10. Trapp T, Rupprecht R, Castren M, Reul JMHM, & Holsboer F (1994) Heterodimerization between mineralocorticoid and glucocorticoid receptor: a new principle of glucocorticoid action in the CNS. *Neuron* 13(6):1457-1462.
11. Savory JG*, et al.* (2001) Glucocorticoid receptor homodimers and glucocorticoid-mineralocorticoid receptor heterodimers form in the cytoplasm through alternative dimerization interfaces. *Mol Cell Biol* 21(3):781-793.
12. Liu W, Wang J, Sauter NK, & Pearce D (1995) Steroid receptor heterodimerization demonstrated in vitro and in vivo. *Proc Natl Acad Sci U S A* 92(26):12480-12484.
13. Jaaskelainen T, Makkonen H, & Palvimo JJ (2011) Steroid up-regulation of FKBP51 and its role in hormone signaling. *Curr Opin Pharmacol* 11(4):326-331.
14. Rawashdeh O*, et al.* (2014) PERIOD1 coordinates hippocampal rhythms and memory processing with daytime. *Hippocampus* 24(6):712-723.
15. Tsai KJ, Chen SK, Ma YL, Hsu WL, & Lee EH (2002) sgk, a primary glucocorticoid-induced gene, facilitates memory consolidation of spatial learning in rats. *Proc Natl Acad Sci U S A* 99(6):3990-3995.
16. Qian X*, et al.* (2011) A rapid release of corticosteroid-binding globulin from the liver restrains the glucocorticoid hormone response to acute stress. *Endocrinology* 152(10):3738-3748.
17. Hubler TR & Scammell JG (2004) Intronic hormone response elements mediate regulation of FKBP5 by progestins and glucocorticoids. *Cell Stress Chaperones* 9(3):243-252.
18. Webster MK, Goya L, Ge Y, Maiyar AC, & Firestone GL (1993) Characterization of sgk, a novel member of the serine/threonine protein kinase gene family which is transcriptionally induced by glucocorticoids and serum. *Mol Cell Biol* 13(4):2031-2040.
19. Itani OA, Liu KZ, Cornish KL, Campbell JR, & Thomas CP (2002) Glucocorticoids stimulate human sgk1 gene expression by activation of a GRE in its 5'-flanking region. *Am J Physiol Endocrinol Metab* 283(5):E971-979.
20. Cheon S, Park N, Cho S, & Kim K (2013) Glucocorticoid-mediated Period2 induction delays the phase of circadian rhythm. *Nucleic Acids Res* 41(12):6161-6174.
21. Binder EB (2009) The role of FKBP5, a co-chaperone of the glucocorticoid receptor in the pathogenesis and therapy of affective and anxiety disorders. *Psychoneuroendocrinology* 34 Suppl 1:S186-195.
22. Bilang-Bleuel A*, et al.* (2005) Psychological stress increases histone H3 phosphorylation in adult dentate gyrus granule neurons: involvement in a glucocorticoid receptor-dependent behavioural response. *Eur J Neurosci* 22(7):1691-1700.
23. Klengel T*, et al.* (2013) Allele-specific FKBP5 DNA demethylation mediates gene-childhood trauma interactions. *Nat Neurosci* 16(1):33-41.
24. Zannas AS & Binder EB (2014) Gene-environment interactions at the FKBP5 locus: sensitive periods, mechanisms and pleiotropism. *Genes Brain Behav* 13(1):25-37.
25. Droste SK*, et al.* (2008) Corticosterone levels in the brain show a distinct ultradian rhythm but a delayed response to forced swim stress. *Endocrinology* 149(7):3244-3253.
26. Miranda TB, Morris SA, & Hager GL (2013) Complex genomic interactions in the dynamic regulation of transcription by the glucocorticoid receptor. *Mol Cell Endocrinol* 380(1-2):16-24.
27. Obradovic D*, et al.* (2004) DAXX, FLASH, and FAF-1 modulate mineralocorticoid and glucocorticoid receptor-mediated transcription in hippocampal cells--toward a basis for the opposite actions elicited by two nuclear receptors? *Mol Pharmacol* 65(3):761-769.
28. Arriza JL, Simerly RB, Swanson LW, & Evans RM (1988) The neuronal mineralocorticoid receptor as a mediator of glucocorticoid response. *Neuron* 1(9):887-900.
29. Website (© 2015 Allen Institute for Brain Science. (Allen Brain Atlas [Internet], Available from http://www.brain-map.org.).
30. De Kloet ER, Vreugdenhil E, Oitzl MS, & Joels M (1998) Brain corticosteroid receptor balance in health and disease. *Endocr Rev* 19(3):269-301.
31. Reul JMHM (2014) Making memories of stressful events: a journey along epigenetic, gene transcription, and signaling pathways. *Front Psychiatry* 5:5.

32. Gutierrez-Mecinas M*, et al.* (2011) Long-lasting behavioral responses to stress involve a direct interaction of glucocorticoid receptors with ERK1/2-MSK1-Elk-1 signaling. *Proc Natl Acad Sci U S A* 108(33):13806-13811.
33. Carter SD, Mifsud KR, & Reul JM (2015) Distinct epigenetic and gene expression changes in rat hippocampal neurons after Morris water maze training. *Front Behav Neurosci* 9:1-13.

Figure legends

Figure 1. hnRNA and mRNA expression of GC-inducible genes in hippocampal sub-regions under baseline conditions and following stress. Rats were either killed direct from home cage (~7am, AM baseline) or at 15 , 30 , 60 or 180 min after the start of FS (15 min, 25°C water). The graphs show expression of *Fkbp5*, *Per1* and *Sgk1* in the dorsal dentate gyrus (A, C, E respectively) or CA regions (B, D, F respectively) and represented as mean fold change over baseline RNA levels (± SEM, n=7-9 per group). Expression of both hnRNA (white bars, left y-axis) and mRNA (black bars, right y-axis) are shown for individual genes. *, $p<0.05$ compared with AM. For more information on statistical analyses in Fig. 1-5, see SI Statistics Information to Main Manuscript Fig. 1-5.

Figure 2. MR and GR binding to GREs within GC-inducible genes in the hippocampus under baseline conditions and following stress. Rats were either killed under AM (~7am) or PM (~5pm) conditions or at 15, 30 , 60 or 180 min after the start of FS (15 min, 25°C water). The graphs show enrichment (Bound/Input (B/I), mean ± SEM, n=3-4) at GREs within *Fkbp5* (A, B), *Per1* (C, D) and *Sgk1* (E, F) after MR and GR ChIP on hippocampal chromatin, respectively. *, $p<0.05$ compared with AM.

Figure 3. Effects of different stressors on MR and GR binding to GC-target genes in the hippocampus. Rats were either killed under baseline AM conditions (BL) or 30 min after stress onset. The graphs show mean enrichment (B/I, ± SEM, n = 8 for baseline group, n=4 for stress groups; FS, forced swimming; NE, novel environment; RS, restraint) at GREs within GC-target genes after MR (A) or GR (B) ChIP on hippocampal chromatin. *, $p<0.05$ compared with respective BL group; ^, $p<0.05$ compared with respective NE group; $^{\$}$, $p<0.05$ compared with respective FS group.

Figure 4. Comparison of MR and GR ChIP on original vs. GR/MR Unbound hippocampal chromatin at the *Fkbp5* GRE2 under baseline conditions and following stress. Rats were either killed under AM or PM conditions or at 30 min after the start of FS (15 min, 25°C water). The graphs show mean enrichment (B/I, ± SEM, n = 3-4/group) at *Fkbp5* GRE2 after (A) MR ChIP on original chromatin (white bars) and on the unbound fraction of chromatin after GR ChIP (black bars) or (B) GR ChIP on original chromatin (white bars) and on the unbound fraction of chromatin after MR ChIP (black bars). *, $p<0.05$ compared with respective ChIP at same time point

Figure 5. Tandem ChIP for MR and GR binding to *Fkbp5* GRE2 in the hippocampus under baseline conditions and following stress. Rats were either killed under AM conditions (BL) or 30 min after the start of FS stress. Graphs show % input (mean ± SEM, n = 3/group) at *Fkbp5* GRE2 after (A) MR ChIP, immediately followed by MR, GR or IgG (negative control) binding to the MR Bound chromatin or (B) GR ChIP, followed by GR, MR or IgG binding to the GR Bound chromatin. The IgG levels (% input) were deducted from the MR and GR Bound data. *, $p<0.05$ compared with respective BL ChIP; $, $p<0.05$ compared with GR → GR FS ChIP.

Figure 1

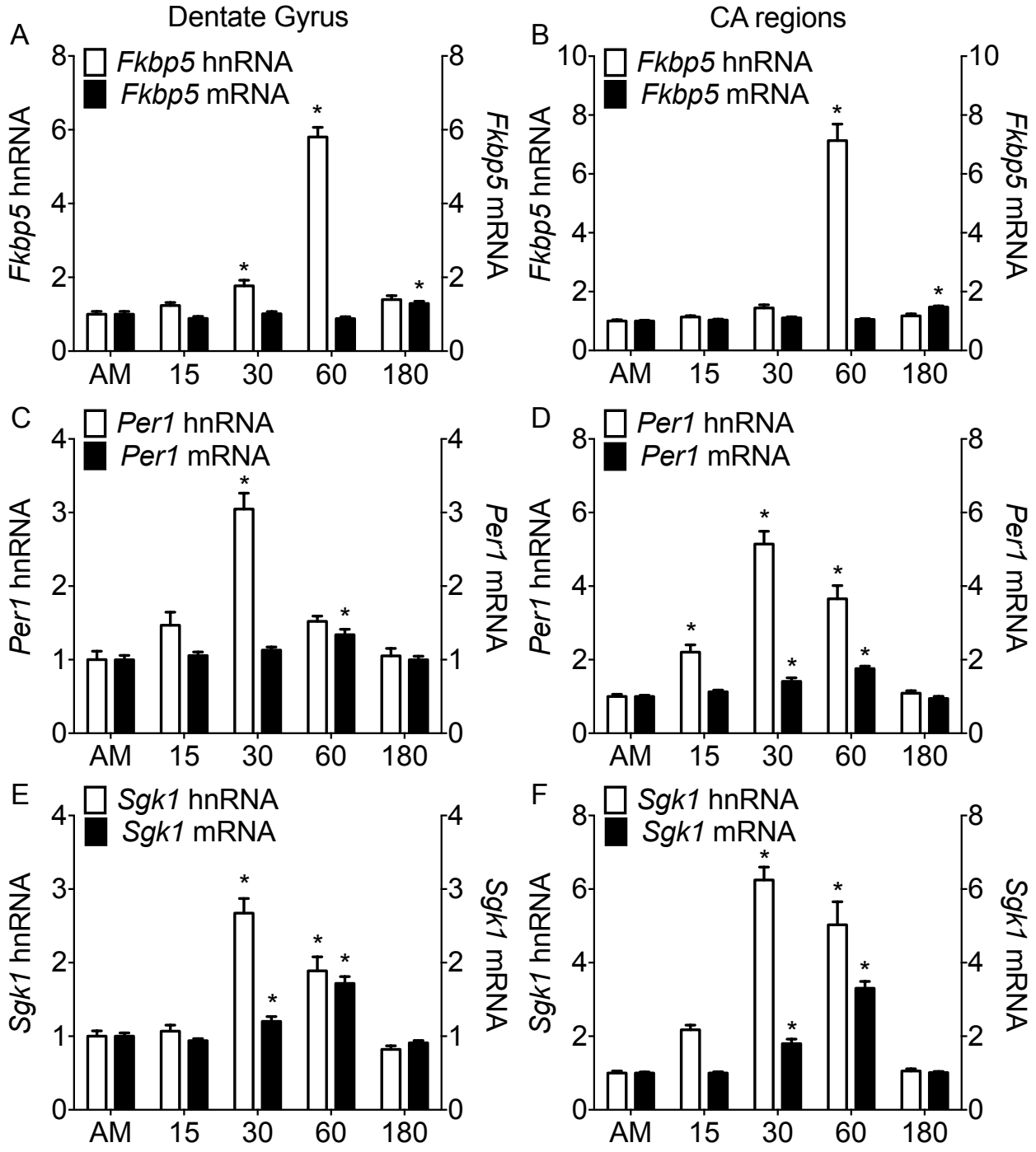
Dentate Gyrus
CA regions
A
B
C
D
E
F
Fkbp5 hnRNA
Fkbp5 mRNA
Per1 hnRNA
Per1 mRNA
Sgk1 hnRNA
Sgk1 mRNA
AM
15
30
60
180

Figure 2

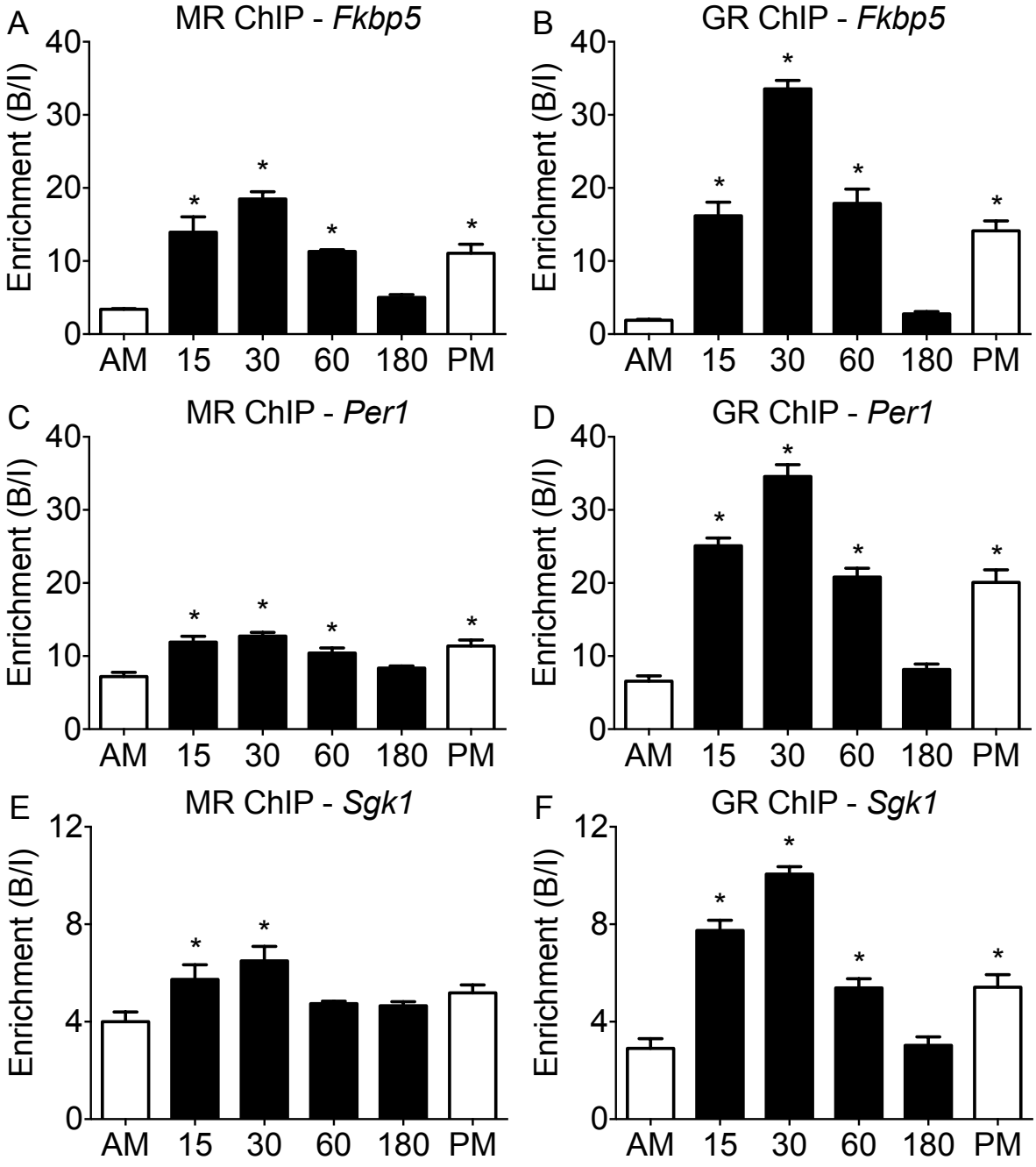
A
MR ChIP - *Fkbp5*
Enrichment (B/I)
0
10
20
30
40
AM
15
30
60
180
PM
B
GR ChIP - *Fkbp5*
C
MR ChIP - *Per1*
D
GR ChIP - *Per1*
E
MR ChIP - *Sgk1*
0
4
8
12
F
GR ChIP - *Sgk1*

Figure 3

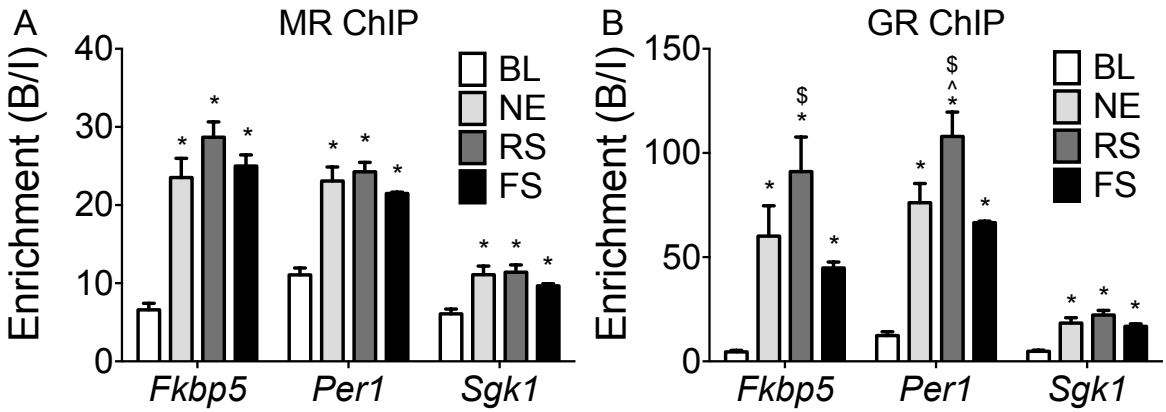
A
MR ChIP
Enrichment (B/I)
40
30
20
10
0
BL
NE
RS
FS
Fkbp5
Per1
Sgk1
B
GR ChIP
Enrichment (B/I)
150
100
50
0
$
^
BL
NE
RS
FS
Fkbp5
Per1
Sgk1

Figure 4

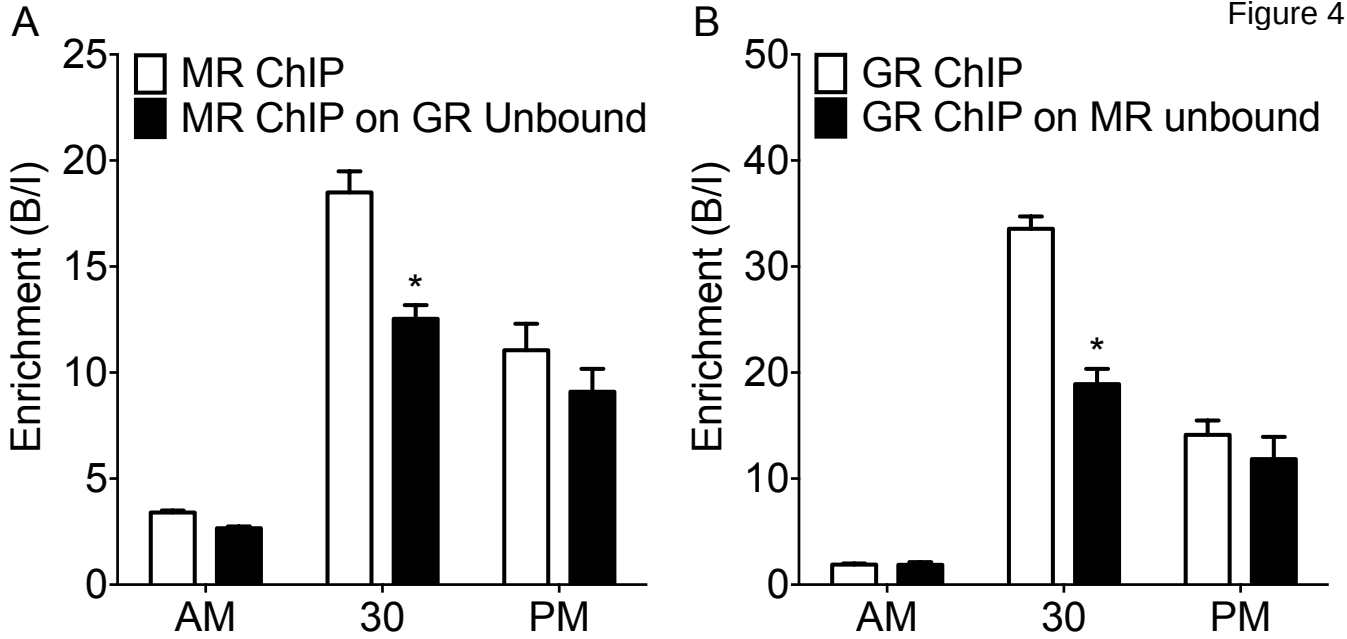
A
MR ChIP
MR ChIP on GR Unbound
Enrichment (B/I)
25
20
15
10
5
0
*
AM
30
PM
B
GR ChIP
GR ChIP on MR unbound
Enrichment (B/I)
50
40
30
20
10
0
*
AM
30
PM

Figure 5

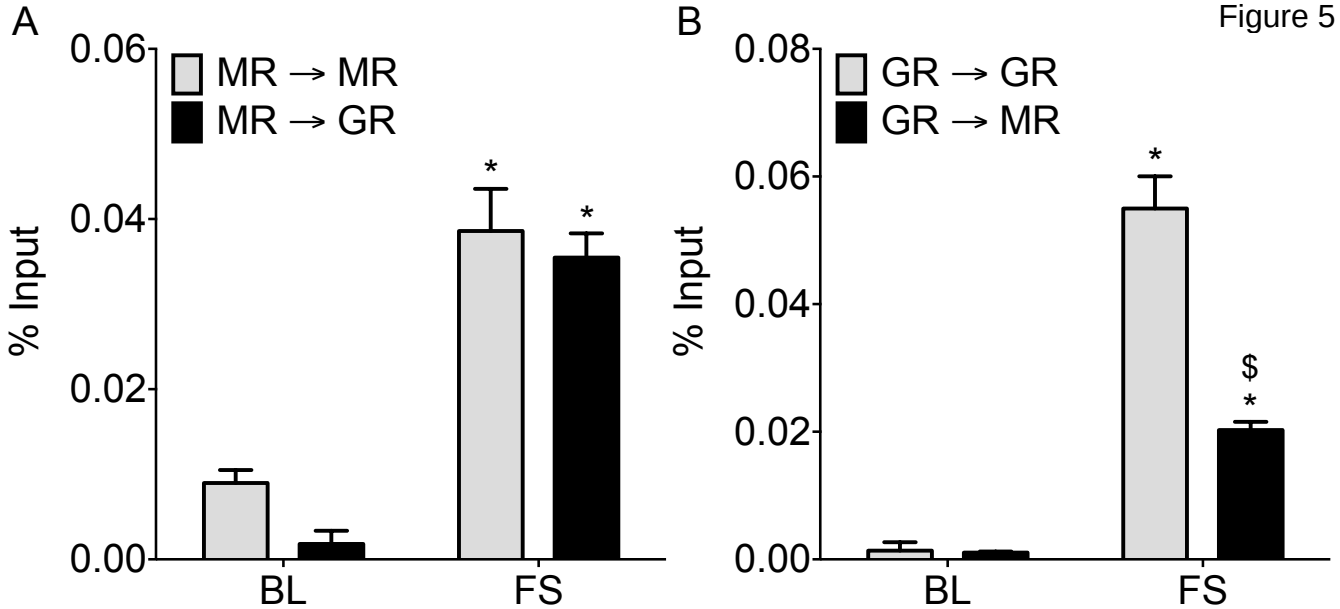
A
0.06
0.04
0.02
0.00
% Input
MR → MR
MR → GR
*
*
BL
FS
B
0.08
0.06
0.04
0.02
0.00
% Input
GR → GR
GR → MR
*
$
*
BL
FS

SI Manuscript file

1. SI Materials and Methods: Page 2-8

2. SI Statistics Information: Pages 9-10
(Extra information (e.g. ANOVA results) on the statistical analyses conducted on the data in the main manuscript figures 1-5)

3. SI Figure legends: Page 11-14
(Legends to the SI Figures S1-S8)

Supporting Information

Mifsud & Reul

1. SI Materials and Methods

Animal experiments

Male Wistar rats were purchased from Harlan (Oxon, UK) weighing 150-175 g upon arrival. Animals were housed 2-3 per cage under standard light (80-100 Lux, lights on 05:00-19:00) and environmentally controlled conditions (temperature 22 ± 2°C; relative humidity 50 ± 10%), food and water available *ad libitum*. After arrival, the animals were given 5 days to habituate to the housing conditions and then handled (2-3 min per rat per day) for a week before the experiment to reduce nonspecific stress. All animal procedures were approved by the University of Bristol Ethical Committee and the Home Office of the United Kingdom (UK Animal Scientific Procedures Act, 1986). Experiments were carried out between 07:00-13:00 as previously described (16, 32). Rats were forced to swim in a glass beaker filled with water at 25°C for 15 min. Rats were then dried and either killed immediately (time point 15 min) or returned to their home cage and killed at 30 min, 60 min or 180 min after the start of forced swimming (FS). Exposure to a novel environment comprised placing the rats individually in a clean, empty, novel cage with increased light intensity (~500 lux) for 30 min. Restraint stress involved placing the rat in a plexiglass restrainer with ventilation holes for 30 min. Immediately after novel environment and restraint stress, rats were killed. Rats were killed quickly by isoflurane (<15 s) exposure followed by decapitation and removal of the brain. For mRNA studies, brains were micro-dissected on ice cold steel boxes as previously described (33) and dorsal DG and CA regions as well as the whole ventral hippocampus samples collected. For whole hippocampal dissections (ChIP studies) brains were also dissected on ice cold steel boxes. All samples were snap-frozen in liquid N_2 and stored at -80°C until analysis. Unless otherwise described all reagents used in sample preparation were from Sigma, Poole UK.

RNA Analysis

RNA was extracted using TRI reagent (Sigma, Poole UK) following manufacturers guidelines. The RNA pellet was air-dried, re-suspended in nuclease-free water (Life Technologies, Paisley, UK) and quantified using a NanoPhotometer P300 (Implen, München, Germany). RNA integrity was assessed in random samples with an Agilent 2100 Bioanalyser to confirm high quality RNA was extracted (RNA integrity numbers (RIN) 8.5 ± 0.1 (mean ± SEM), n=12). Total RNA was reverse transcribed into cDNA using the QuantiTect reverse transcription kit (Qiagen, Manchester, UK) as per manufacturer's instructions (15 min, 42°C; 5 min, 95°C) using a BioRad T1000 thermal cycler. cDNA was diluted 4-fold and 2 µl of diluted cDNA was used per reaction in quantitative polymerase chain reaction (qPCR) analysis detailed below. Expression of mRNA in samples was calculated based on the Pfaffl method of relative quantification (33) using primer/probes listed in Table S1 and standardised to the expression of housekeeping genes hypoxanthine phosphoribosyltransferase 1 (*Hprt1*) and tyrosine 3-monooxygenase/tryptophan 5-monooxygenase activation protein, zeta (*Ywhaz*). The data were expressed as fold change over baseline.

qPCR analysis

Mastermix for qPCR was prepared containing 900 nM forward and reverse primers, 200 nM probe, 1X TaqMan fast mastermix (Life Technologies, Paisley, UK) and made up to volume with nuclease-free water. Primers and dual-labelled probe with 6-FAM as the fluorescent dye and TAMRA as the quencher were designed using Primer Express software (Version 3.0.1, Life Technologies) (Table S1). Standard curves were performed for each primer pair and the qPCR efficiency was calculated using the equation: E = (10-1/slope) – 1) x 100 (where E is qPCR efficiency and the slope is the gradient of the standard curve). Only primer pairs with efficiencies greater that 90% were used. Quantitative

PCR was performed using a StepOne Plus machine (Life Technologies, Paisley, UK). Taq enzymes were activated at 95°C for 20 s, then 40 cycles of 95°C (1 s) to 60°C (20 s) were performed to amplify samples.

Chromatin preparation and chromatin immunoprecipitation (ChIP) analysis

Standard ChIP was performed as previously described (33). We added 1 mM AEBSF or 0.1 mM PMSF, 5mM Na^+-Butyrate (NaBut), and PhosSTOP phosphatase inhibitor cocktail tablets (1 per 10 ml; Roche, Burgess Hill, UK) to all solutions unless otherwise stated. Briefly, hippocampal tissues from two rats were cross-linked for 10 min in 1% formaldehyde in PBS. Crosslinking was terminated by adding glycine (5 min, final concentration 200 µM) and centrifuged (5 min, 6000 g, 4°C). Pellets were washed three times with ice-cold PBS. Next, the pellets were re-suspended in ice-cold Lysis Buffer [50 mM Tris-HCl pH 8, 150 mM NaCl, 5mM EDTA pH 8.0, 0.5% v/v Igepal, 0.5% Na-deoxycholate, 1% SDS, 5mM NaBut, 2 mM AEBSF, 1mM Na3VO4, Complete ultra EDTA-free protease inhibitor tablets and PhosSTOP phosphatase inhibitor cocktail tablet (both 1 per 10 ml, Roche, Burgess Hill, UK)] and rotated for 15 min at 4°C. Samples were aliquoted, sonicated (high power; 3 x 10 cycles; 30 s ON, 60 s OFF) using a water-cooled (4°C) Bioruptor (UCD-300, Diagenode, Liège, Belgium) and centrifuged (10 min, 20,000 g, 4°C). Supernatants (containing the sheared chromatin) were recombined and re-aliquoted into fresh tubes for subsequent ChIP analysis and for assessment of Input DNA (i.e. the starting material). Chromatin was sonicated to approximately 3-nucleosome lengths (approximately 450 bp), as confirmed by agarose gel electrophoresis (Fig. S7).

For ChIP analysis, aliquots of chromatin were diluted 10-times in ice-cold Dilution Buffer [50 mM Tris-HCl pH 8.0, 150 mM NaCl, 5 mM EDTA pH 8.0, 1% v/v Triton, 0.1% Na-deoxycholate 5mM NaBut, 1 mM AEBSF, Complete Ultra EDTA-free protease inhibitor tablets and PhosSTOP phosphatase inhibitor cocktail tablet (both 1 per 10 ml, Roche)]. 10 µl of antibody, either MR (MR H-300 antibody;

sc11412X; Santa Cruz, USA), GR (sc8992X; Santa Cruz) or IgG control (GR H-300 antibody; sc2027X; Santa Cruz) was added to each sample and tubes were rotated overnight at 4°C. The anti-MR and anti-GR antibodies were checked for specificity by Western blotting (Fig. S8A) and have been used in published studies (8, 9). In addition, we conducted ChIP assays with alternative MR and GR antibodies (MR N-17 (sc-6860X, Santa Cruz); GR M-20 (sc-1004X, Santa Cruz) on baseline AM and FS30 hippocampal chromatin producing similar results to those obtained previously with the MR H-300 and GR H-300 antibodies (Fig. S8B). Pre-absorption tests using preparations of peptide (MR-peptide (sc-6860 P); GR-peptide (sc-1004 P)) against which the antibodies MR N-17 and GR M-20 had been raised were performed as well (Fig. S8B). These control experiments demonstrated that the MR and GR antibodies showed selective specificity for the respective receptor against which they had been produced. The IgG antibody (normal rabbit control IgG, sc-2027X, Santa Cruz) was used to check for non-specific binding. As shown in SI Figure S8C, the IgG ChIP resulted in an enrichment virtually equalling 1 (B/I ≈1) indicating no significant non-specific binding. Protein A-coated Dynabeads® (Life Technologies; for MR N-17 antibody, Protein G-coated Dynabeads® were used) were washed once in ice-cold 0.5% BSA/PBS before blocking overnight at 4°C. Pre-blocked beads were washed once in ice-cold Dilution buffer, re-suspended in the antibody:chromatin mix, and allowed to incubate for 3 h at 4°C to allow binding of beads to antibody:chromatin complexes. After 3 h, the samples were placed in a magnetic stand to allow the beads (with the Bound fraction bound) to separate from the liquid 'Unbound' fraction. In some ChIP assays, this Unbound fraction was collected in separate tubes for additional ChIP assays. In these assays, anti-MR antibody was added to chromatin that had been previously incubated with anti-GR antibody (a GR Unbound fraction), vice versa, anti-GR antibody was added to an MR Unbound fraction. After addition of antibody, ChIP on Unbound fraction proceeded as usual.

Beads carrying the Bound chromatin were washed 3-times with ice-cold RIPA buffer [10 mM Tris-HCl pH 7.5, 1 mM EDTA pH 7.5, 0.1% SDS, 0.5 mM EGTA, 1% Triton, 0.1% Na-Deoxycholate, 140 mM NaCl + inhibitors] and washed twice with ice-cold Tris-EDTA buffer. Bound DNA was eluted in two

steps at room temperature; first with 200 µl Elution buffer 1 (10 mM Tris-HCl pH 7.4, 50 mM NaCl, 1.5% SDS) and second with 100 µl Elution buffer 2 (10 mM Tris-HCl pH 7.4, 50 mM NaCl, 0.5% SDS). Crosslinks were reversed by addition of NaCl (final concentration 200 mM) and overnight incubation at 65°C. The next day, samples were incubated first with RNase A (60 µg/ml, 37°C, 1 h), followed by incubation with proteinase K (250 µg/ml, 37°C, 3.5 h). DNA was purified using a QIAquick PCR purification kit (Qiagen) as per manufacturer's instructions. Input samples were incubated overnight at 65°C with 200 mM NaCl to reverse crosslinks, incubated with RNase A and proteinase K (overnight), and DNA was purified using a Qiagen PCR purification kit. Total double-stranded DNA (dsDNA) content was determined with a high-sensitivity Qubit DNA assay kit (Life Technologies) as per manufacturer's instructions and quantified using a Qubit 2.0 fluorometer. All samples (Bounds and Inputs) were diluted to a standardised concentration with nuclease free water and analysed by qPCR as described above using primers/probes listed in Table S1. A standard curve, created from serial dilutions of rat brain genomic DNA (Biochain, CA, USA), was included in each qPCR run. Data are expressed as quantity of bound DNA divided by the respective quantity of input DNA, i.e. Bound/Input (B/I), which is a measure of the enrichment of steroid receptor bound to specific genomic sequences.

For Tandem ChIP the protocol of ChIP explained above was used albeit with modifications. To attain n=3 independent samples, three pools of chromatin were prepared of hippocampus tissue from 4 rats (baseline or killed 30min after FS) for each pool. From each pool of chromatin, aliquots were incubated with anti-GR H300 antibody overnight at 4 C after which the mixture was incubated for 3 h with Protein A-coated Dynabeads at 4 C. Subsequently, the beads were washed as described above and, next, incubated with 1% SDS buffer (50 mM Tris, 10 mM EDTA, 1% SDS) at 68°C for 15 min. After incubation in this hot SDS buffer, samples were allowed to cool and were then diluted 10-times in ice-cold Dilution buffer. The samples were placed in ice and either 10 µl anti-GR H-300 (GR → GR), anti-MR H300 (GR → MR) or anti-IgG (=background control; GR → IgG) antibody was added to start the second ChIP. After overnight incubation at 4 C, the mixture was incubated with protein A-coated

Dynabeads, which were subsequently washed and eluted, as described for the normal ChIP protocol above.

In a separate Tandem ChIP assay, for the reverse protocol, aliquots of chromatin (n=3) were incubated first with anti-MR antibody (1st ChIP) and subsequently with either anti-MR (MR → MR), anti-GR (MR → GR) or anti-IgG (MR → IgG) antibody (2nd ChIP).

The amount of recovered DNA (after reversal of crosslinks, RNase and proteinase K treatment and purification using Qiagen PCR purification columns) was too low to quantify using the Qubit dsDNA assay kit used above. Therefore, equal volumes of Bound and Input samples were subjected to qPCR using the GRE-spanning primers for the three genes (*Fkbp5, Per1, Sgk1*) listed in Table S1. Binding was then calculated as percentage of Input (%Input). The %Input values of the GR → IgG and MR → IgG ChIP samples were deducted from the values of the respective GR and MR Tandem ChIP outcomes.

Western blotting

Hippocampal nuclear and cytoplasmic fractions were prepared using Universal Magnetic co-immunoprecipitation (co-IP) kit (Active Motif, Belgium) according to manufacturer's instructions. Protein was quantified using Qubit protein assay kit (Life Technologies) as per manufacturer's instructions using a Qubit 2.0. Nuclear protein samples (20 µg per well) and Precision Plus Protein™ Dual Color Standard protein ladder (BioRad, UK) were loaded onto 4-15% Mini-PROTEAN® TGX™ Precast Gels (BioRad, UK) and separated by electrophoresis for ~45 min at 200V. Proteins were transferred to a PVDF membrane (BioRad, UK) and blocked overnight (GR: 5% BSA/PBS-T; MR: 5% milk/PBS-T) at 4°C. Membranes were incubated with either anti-GR (H-300, sc-8992X, Santa Cruz, Germany, 1:500) or anti-MR (H-300, sc-11412X, Santa Cruz, Germany, 1:500) in 1% blocking solution for 2 h at room temperature. Membranes were washed three times (PBS-T) and incubated with goat

αRb horseradish peroxidase- (HRP; Jackson ImmunoResearch, Suffolk, UK. 1:5000 in 0.5% blocking solution) for 1 h then finally washed a further five times. Antibody binding was visualised by enhanced chemiluminescence (ECL) using reagents (GE healthcare, Amersham, UK) and processor (G-Box, Syngene, UK) following the manufacturers guidelines.

Measurement of corticosterone by radioimmunoassay (RIA)

Plasma CORT concentrations were measured using a commercial CORT RIA kit (MP Biomedicals, Solon, OH) as described previously (16).

Statistical analysis

Data were statistically analyzed using SPSS (IBM). Results are presented as group means ± SEM; sample sizes are indicated in the figure legends. Multiple statistical comparisons were conducted with one-way or two-way ANOVA and if significant, a Bonferroni post hoc test was performed. Statistical results are provided in the figure legends. $P<0.05$ was considered statistically significant.

2. SI Statistics Information to Main Manuscript Figs. 1-5

Heteronuclear and mature RNA expression of glucocorticoid-inducible genes in hippocampal sub-regions under baseline conditions and following stress (Fig. 1). Statistical analysis was as follows: One-way ANOVA: (A) hnRNA $F_{(4, 38)} = 167.50$, $p < 0.0001$; mRNA $F_{(4, 38)} = 7.97$, $p < 0.0001$ (B) hnRNA $F_{(4, 39)} = 102.10$, $p < 0.0001$; mRNA $F_{(4, 39)} = 35.02$, $p < 0.0001$ (C) hnRNA $F_{(4, 37)} = 32.87$, $p < 0.0001$; mRNA $F_{(4, 38)} = 6.45$, $p < 0.0001$ (D) hnRNA $F_{(4, 37)} = 50.23$, $p < 0.0001$; mRNA $F_{(4, 36)} = 25.07$, $p < 0.0001$ (E) hnRNA $F_{(4, 38)} = 32.12$, $p < 0.0001$; mRNA $F_{(4, 36)} = 37.50$, $p < 0.0001$ (F) hnRNA $F_{(4, 39)} = 51.28$, $p < 0.0001$; mRNA $F_{(4, 39)} = 97.56$, $p < 0.0001$. Bonferroni post hoc test: *, $p<0.05$ compared with early morning baseline (AM).

Analysis of MR and GR binding to GREs within glucocorticoid-inducible genes in the hippocampus under baseline conditions and following stress (Fig. 2). Statistical analysis was as follows: One-way ANOVA: (A) $F_{(5, 17)} = 27.88$, $p < 0.0001$ (B) $F_{(5, 17)} = 68.19$, $p < 0.0001$ (C) $F_{(5, 17)} = 11.94$, $p < 0.0001$ (D) $F_{(5, 17)} = 66.62$, $p < 0.0001$ (E) $F_{(5, 17)} = 4.49$, $p = 0.0086$ (F) $F_{(5, 17)} = 45.44$, $p < 0.0001$. Bonferroni post hoc test: *, $p<0.05$ compared with early morning baseline (AM).

Effects of different stressors on MR and GR receptor binding to glucocorticoid-inducible genes in the hippocampus (Fig. 3). Statistical analysis was as follows: One-way ANOVA: (A) *Fkbp5,* $F_{(3, 16)} = 52.81$, $p < 0.0001$; *Per1,* $F_{(3, 16)} = 36.74$, $p < 0.0001$; *Sgk1,* $F_{(3, 16)} = 12.35$, $p < 0.0001$ (B) *Fkbp5,* $F_{(3, 16)} = 19.79$, $p < 0.0001$; *Per1,* $F_{(3, 16)} = 52.37$, $p < 0.0001$; *Sgk1,* $F_{(3, 16)} = 32.35$, $p < 0.0001$. Bonferroni post hoc test: *, $p<0.05$ compared with respective BL group; ^, $p<0.05$ compared with respective NE group; $^{\$}$, $p<0.05$ compared with respective FS group.

Comparison of MR and GR binding to different GRE sites in the *Fkbp5* gene in the hippocampus (Fig. 4). Statistical analysis was as follows: Two-way ANOVA: (A) effect of stress: $F_{(1, 12)} = 88.07$, $p < 0.0001$; effect of GRE location $F_{(1, 12)} = 134.60$, $p < 0.0001$; interaction stress x GRE location $F_{(1, 12)} = 69.07$, $p < 0.0001$ (B) effect of stress: $F_{(1, 12)} = 180.40$, $p < 0.0001$; effect of GRE location $F_{(1, 12)} = 193.10$, $p < 0.0001$; interaction stress x GRE location $F_{(1, 12)} = 146.60$, $p < 0.0001$. Bonferroni post hoc test: *, $p<0.05$ compared with respective BL group.

Comparison of MR and GR ChIP on original versus GR/MR Unbound hippocampal chromatin at an intronic GRE within the *Fkbp5* gene under baseline conditions and following stress (Fig. 5). Statistical analysis was as follows: Two-way ANOVA (A) effect of stress: $F_{(2, 18)} = 114.40$, $p < 0.0001$; effect of ChIP $F_{(1, 18)} = 18.24$, $p < 0.0005$; interaction stress x ChIP $F_{(2, 18)} = 5.440$, $p = 0.0142$ (B) effect of stress: $F_{(2, 18)} = 183.60$, $p < 0.0001$; effect of ChIP $F_{(1, 18)} = 29.57$, $p < 0.0001$; interaction stress x ChIP $F_{(2, 18)} = 19.11$, $p < 0.0001$. Bonferroni post hoc test: *, $p<0.05$ compared with respective ChIP at same time point.

Tandem ChIP for MR and GR binding to GRE2 within *Fkbp5* in the hippocampus under baseline conditions and following stress (Fig. 6). Statistical analysis was as follows: Two-way ANOVA: (A) effect of stress: $F_{(1, 8)} = 112.77$, $p < 0.0001$; effect of ChIP $F_{(1, 8)} = 2.97$, $p = 0.123$; interaction stress x ChIP: $F_{(1, 8)} = 0.46$, $p = 0.517$ (B) effect of stress: $F_{(1, 8)} = 191.52$, $p < 0.0001$; effect of ChIP $F_{(1, 8)} = 44.26$, $p = 0.0002$; interaction stress x ChIP: $F_{(1, 8)} = 42.79$, $p = 0.0002$. Bonferroni post hoc test: *, $p<0.05$ compared with respective BL ChIP; $, $p<0.05$ compared with GR → GR FS ChIP.

3. SI Figure Legends

Figure S1. Heteronuclear and mature RNA expression of glucocorticoid-inducible genes in the ventral hippocampus under baseline conditions and following stress. Rats were either killed direct from home cage (~7am, AM baseline) or at 15 min (15), 30 min (30), 60 min (60) or 180 mins (180) after the start of forced swimming (15 min, 25°C water). The graphs show expression of *Fkbp5*, *Per1* and *Sgk1* in the ventral hippocampus (A-C, respectively) after normalisation to the expression of housekeeping genes *Hprt1* and *Ywhaz* and represented as mean fold change over baseline RNA levels (± SEM, n=8-9 per group). Expression of both heteronuclear RNA (white bars, left y-axis) and mature RNA (black bars, right y-axis) are shown for individual genes. Statistical analysis: One-way ANOVA: (A) hnRNA $F_{(4, 35)} = 155.30$, $p < 0.0001$; mRNA $F_{(4, 35)} = 23.13$, $p < 0.0001$ (B) hnRNA $F_{(4, 35)} = 66.36$, $p < 0.0001$; mRNA $F_{(4, 34)} = 12.67$, $p < 0.0001$ (C) hnRNA $F_{(4, 36)} = 42.22$, $p < 0.0001$; mRNA $F_{(4, 35)} = 60.10$, $p < 0.0001$. Bonferroni post hoc test: *, $p<0.05$ compared with baseline (AM).

Figure S2. Plasma corticosterone levels under baseline conditions and following stress. Plasma corticosterone levels (ng/ml, mean ± SEM) from baseline rats killed direct from home cage in early morning (~7am, AM baseline) or late afternoon (~5pm, PM baseline) or rats killed 15 min (15), 30 min (30), 60 min (60) or 180 mins (180) after the start of forced swimming (15 min, 25°C water) are shown. Statistical analysis: One-way ANOVA: $F_{(5, 51)} = 284.6$, $p < 0.0001$. Bonferroni post hoc test: *, $p<0.05$ compared with early morning baseline (AM).

Figure S3. Gene maps of glucocorticoid-inducible genes. The location of GREs within the rat glucocorticoid target genes *Fkbp5*, *Per1* and *Sgk1* are shown. Gene traces were adapted from the Rnor_6.0 assembly (http://genome.ucsc.edu/).

Figure S4. Comparison of MR and GR binding to different GRE sites in the *Fkbp5* gene in the hippocampus. Rats were either killed direct from home cage under baseline AM conditions (BL) or 30 min after the start forced-swim stress. The graphs show mean enrichment (B/I, ± SEM, n = 4/group) at differential GREs within the *Fkbp5* gene after MR (A) or GR (B) ChIP on hippocampal chromatin. Statistical analysis: Two-way ANOVA: (A) effect of stress: $F_{(1, 12)} = 88.07$, $p < 0.0001$; effect of GRE location $F_{(1, 12)} = 134.60$, $p < 0.0001$; interaction stress x GRE location $F_{(1, 12)} = 69.07$, $p < 0.0001$ (B) effect of stress: $F_{(1, 12)} = 180.40$, $p < 0.0001$; effect of GRE location $F_{(1, 12)} = 193.10$, $p < 0.0001$; interaction stress x GRE location $F_{(1, 12)} = 146.60$, $p < 0.0001$. Bonferroni post hoc test: *, $p<0.05$ compared with respective BL group

Figure S5. Comparison of MR and GR ChIP on original versus GR/MR Unbound hippocampal chromatin at GREs within glucocorticoid-inducible genes under baseline conditions and following stress. Rats were either killed direct from home cage in early morning (~7am, AM baseline) or late afternoon (~5pm, PM baseline) or at 30 min after the start of forced swimming (15 min, 25°C water). The graphs show mean enrichment (Bound/Input, ± SEM, n = 3-4/group) of GREs within the *Per1* (A, B) or *Sgk1* (C, D) genes after MR ChIP on original chromatin (white bars) and on the unbound fraction of chromatin after GR ChIP (black bars) or GR ChIP on original chromatin (white bars) and on the unbound fraction of chromatin after MR ChIP (black bars) respectively. Two-way ANOVA (A) effect of stress: $F_{(2, 16)} = 25.92$, $p < 0.0001$; effect of ChIP $F_{(1, 16)} = 0.53$, $p = 0.4774$; interaction stress x ChIP: $F_{(2, 16)} = 2.04$, $p = 0.1624$ (B) effect of stress: $F_{(2, 16)} = 36.45$, $p < 0.0001$; effect of ChIP: $F_{(1, 16)} = 4.07$, $p = 0.0587$; interaction stress x ChIP: $F_{(2, 16)} = 1.702$, $p = 0.2104$ (C) effect of stress: $F_{(2, 17)} = 17.88$, $p < 0.0001$; effect of ChIP: $F_{(1, 17)} = 2.31$, $p = 0.1471$; interaction stress x ChIP: $F_{(2, 17)} = 1.79$, $p = 0.1978$ (D) effect of stress: $F_{(2, 17)} = 37.66$, $p < 0.0001$; effect of ChIP: $F_{(1, 17)} = 8.48$, $p = 0.0093$; interaction

stress x ChIP: $F_{(2, 17)} = 3.325$, $p = 0.0590$. Bonferroni post hoc test: *, $p<0.05$ compared with respective ChIP at same time point

Figure S6. Tandem ChIP for MR and GR binding to GREs within *Per1* and *Sgk1* in the hippocampus under baseline conditions and following stress. Rats were either killed direct from home cage under baseline AM conditions (BL) or 30 min after the start of forced swim (FS) stress. Graphs show binding (%input ± SEM, n = 3 per group) at specific GREs within the *Per1* (A, B) and *Sgk1* (C, D) genes after (A, C) MR ChIP, immediately followed by MR, GR or IgG (negative control) binding to the MR Bound chromatin or (B, D) GR ChIP, followed by GR, MR or IgG (negative control) binding to the GR Bound chromatin. The IgG levels (% input) were deducted from the MR and GR Bound data. Two-way ANOVA: (A) MR ChIP – *Per1*: effect of stress: $F_{(1, 8)} = 91.56$, $p < 0.0001$; effect of ChIP $F_{(1, 8)} = 50.37$, $p = 0.0001$; interaction stress x ChIP: $F_{(1, 8)} = 0.60$, $p = 0.4622$ (B) GR ChIP – *Per1:* effect of stress: $F_{(1, 8)} = 997.34$, $p < 0.0001$; effect of ChIP $F_{(1, 8)} = 1032.59$, $p < 0.0001$; interaction stress x ChIP: $F_{(1, 8)} = 815.8$, $p < 0.0001$ (C) MR ChIP – *Sgk1:* effect of stress: $F_{(1, 8)} = 12.88$, $p = 0.0071$; effect of ChIP: $F_{(1, 8)} = 8.09$, $p = 0.0217$; interaction stress x ChIP: $F_{(1, 8)} = 1.68$, $p = 0.2316$ (D) GR ChIP – *Per1:* effect of stress: $F_{(1, 8)} = 239.38$, $p < 0.0001$; effect of ChIP: $F_{(1, 8)} = 287.04$, $p < 0.0001$; interaction stress x ChIP: $F_{(1, 8)} = 216.98$, $p < 0.0001$. Bonferroni post hoc test: *, $p<0.05$ compared with respective BL ChIP; $, $p<0.05$ compared with GR → GR FS ChIP.

Figure S7. Confirmation of the sonication efficiency in reversed and non-reversed hippocampal chromatin. This figure shows a representative blot of sheared hippocampal chromatin from all forced swim time course groups before (odd number) or after (even numbers) reversal of crosslinks. Well allocations: 1 & 2, Baseline AM; 3 & 4, FS15; 5 & 6, FS30; 7 & 8, FS60; 9 & 10, FS180; 11 & 12, Baseline PM.

Figure S8. Antibody specificity control experiments. A. Western blot analysis of the GR H-300 (upper image) and MR H-300 (lower image) antibodies. From left: lanes 1 & 2: nuclear fractions of FS30 hippocampus tissue; lane 3: protein ladder under UV illumination; lane 4: ladder under normal light. The ladder contains markers at 75 and 100 kDa. The lanes containing the nuclear fractions show bands generated by the GR antibody and the MR antibody at approximately 92 and 103 kDa, respectively, which corresponds with the predicted protein molecular weights. There was no cross-over in the staining pattern as the GR antibody did not visualize a protein band at 103 kDa and the MR antibody did not recognize a band at 92 kDa. **B.** Pre-absorption analysis and ChIP on hippocampal chromatin using MR N-17 and GR M-20 antibodies. Chromatin was prepared from rats killed under baseline AM conditions (BL) of at 30 min after FS (FS30). Aliquots of MR N-17 and GR M-20 antibody were pre-incubated with peptide preparations against which the antibodies had been raised for 3 hrs at 4°C, as indicated in (B). Next, the antibody-peptide mixture was added to chromatin samples and the ChIP procedure continued as described. qPCR analysis of Bound DNA was conducted using primers for *Fkbp5* GRE2. Data are expressed as Bound/Input (B/I), mean ± SEM; n=3. Statistical analysis: Two-way ANOVA: MR (left panel): Effect of stress: $F_{(1, 12)}$=244.1, P<0.0001; Effect of antibody treatment: $F_{(2, 12)}$=88.63, P<0.0001; Interaction: $F_{(2, 12)}$=57.82, P<0.0001. GR (right panel): Effect of stress: $F_{(1, 12)}$=119.8, P<0.0001; Effect of antibody treatment: $F_{(2, 12)}$=32.7, P<0.0001; Interaction: $F_{(2, 12)}$=29.64, P<0.0001. Bonferroni post hoc test: *, P<0.05, compared with the respective BL control. **C.** IgG binding to *Fkbp5* GRE2 under baseline conditions and following stress. ChIP with normal IgG antibody was conducted with hippocampal chromatin prepared from rats killed under baseline AM or PM conditions or at 30 min after FS. The graph shows lack of IgG enrichment (B/I, mean ± SEM; n=3) at *Fkbp5* GRE2 under all conditions. Statistical analysis: One-way ANOVA: $F_{(2, 8)} = 0.7582$, $p = 0.5087$.

Figure S1

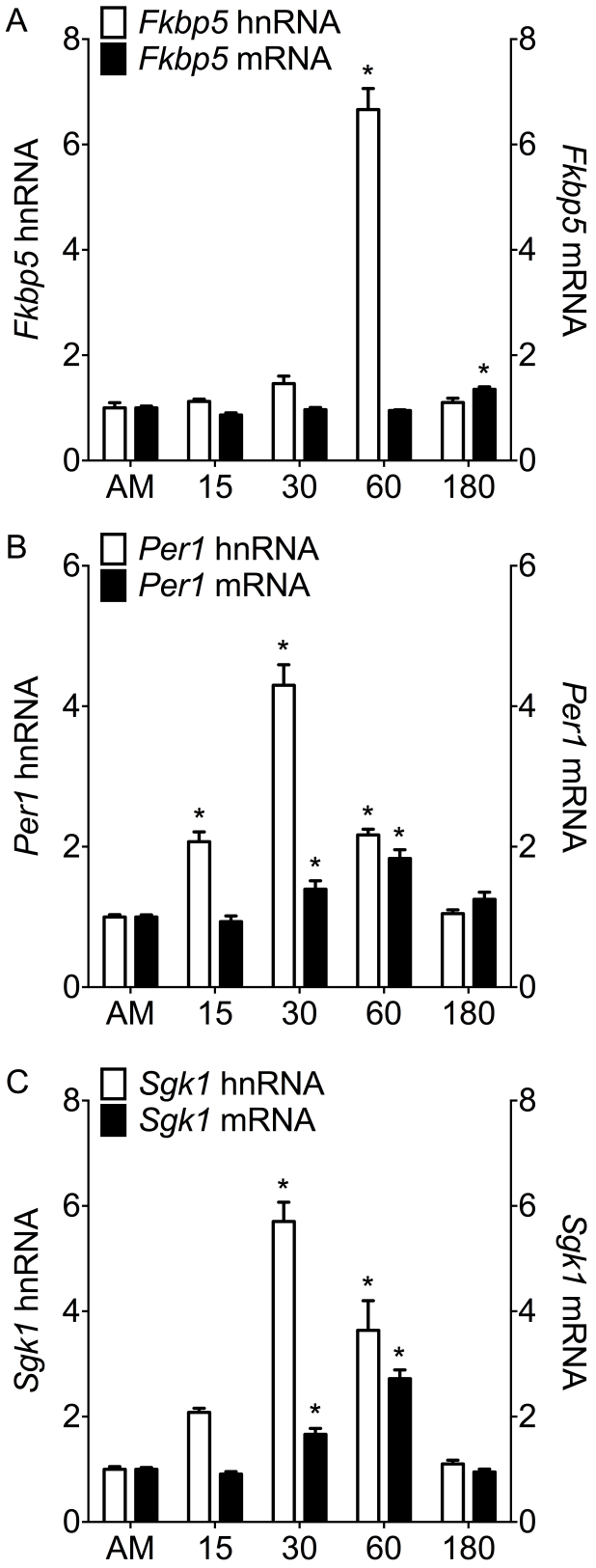
A
Fkbp5 hnRNA
Fkbp5 mRNA
Fkbp5 hnRNA
Fkbp5 mRNA
0
2
4
6
8
AM
15
30
60
180
B
Per1 hnRNA
Per1 mRNA
Per1 hnRNA
Per1 mRNA
0
2
4
6
AM
15
30
60
180
C
Sgk1 hnRNA
Sgk1 mRNA
Sgk1 hnRNA
Sgk1 mRNA
0
2
4
6
8
AM
15
30
60
180

Figure S2

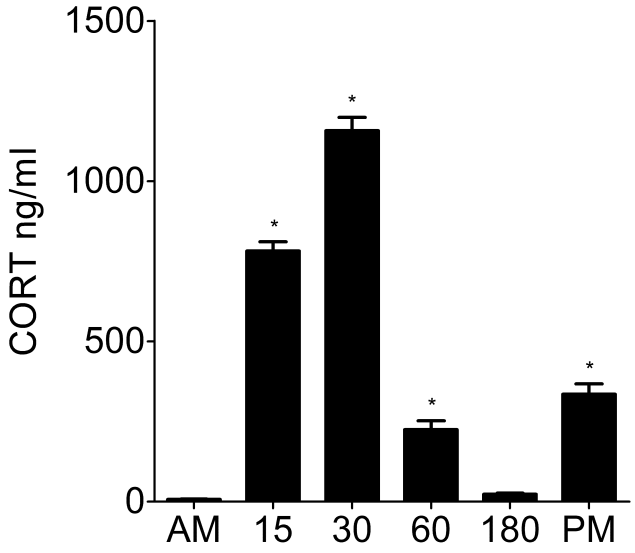

Figure S3

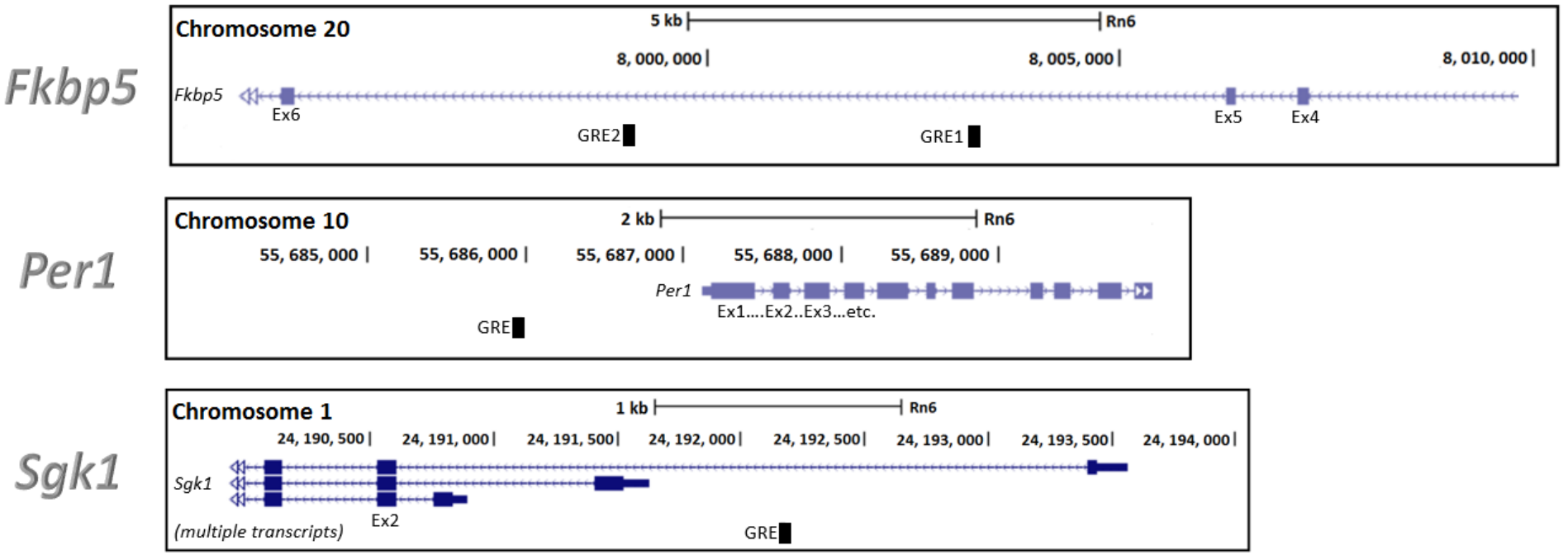
Fkbp5
Chromosome 20
5 kb
Rn6
8, 000, 000
8, 005, 000
8, 010, 000
Fkbp5
Ex6
Ex5
Ex4
GRE2
GRE1
Per1
Chromosome 10
2 kb
Rn6
55, 685, 000
55, 686, 000
55, 687, 000
55, 688, 000
55, 689, 000
Per1
Ex1....Ex2..Ex3...etc.
GRE
Sgk1
Chromosome 1
1 kb
Rn6
24, 190, 500
24, 191, 000
24, 191, 500
24, 192, 000
24, 192, 500
24, 193, 000
24, 193, 500
24, 194, 000
Sgk1
(multiple transcripts)
Ex2
GRE

Figure S4

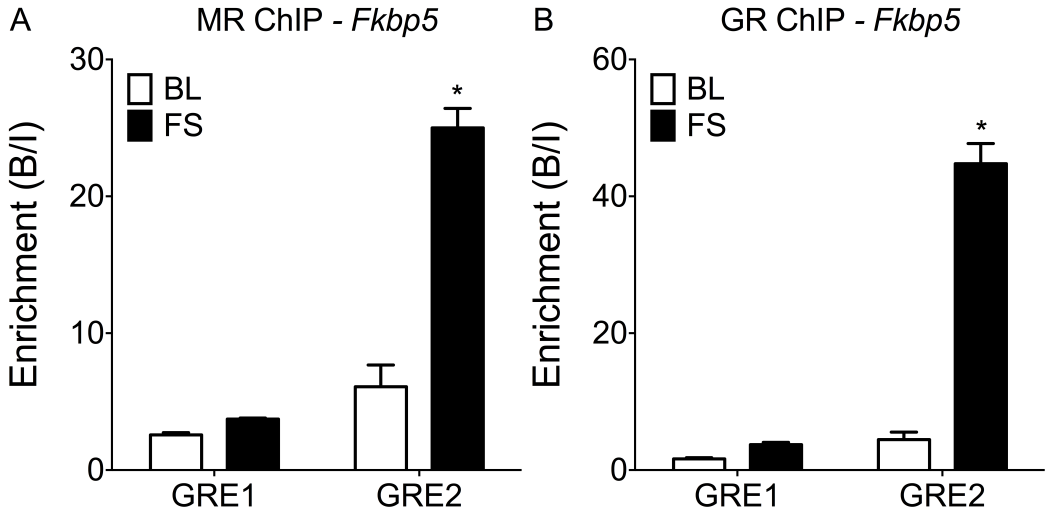
A
MR ChIP - Fkbp5
Enrichment (B/I)
30
20
10
0
BL
FS
*
GRE1
GRE2
B
GR ChIP - Fkbp5
Enrichment (B/I)
60
40
20
0
BL
FS
*
GRE1
GRE2

Figure S5

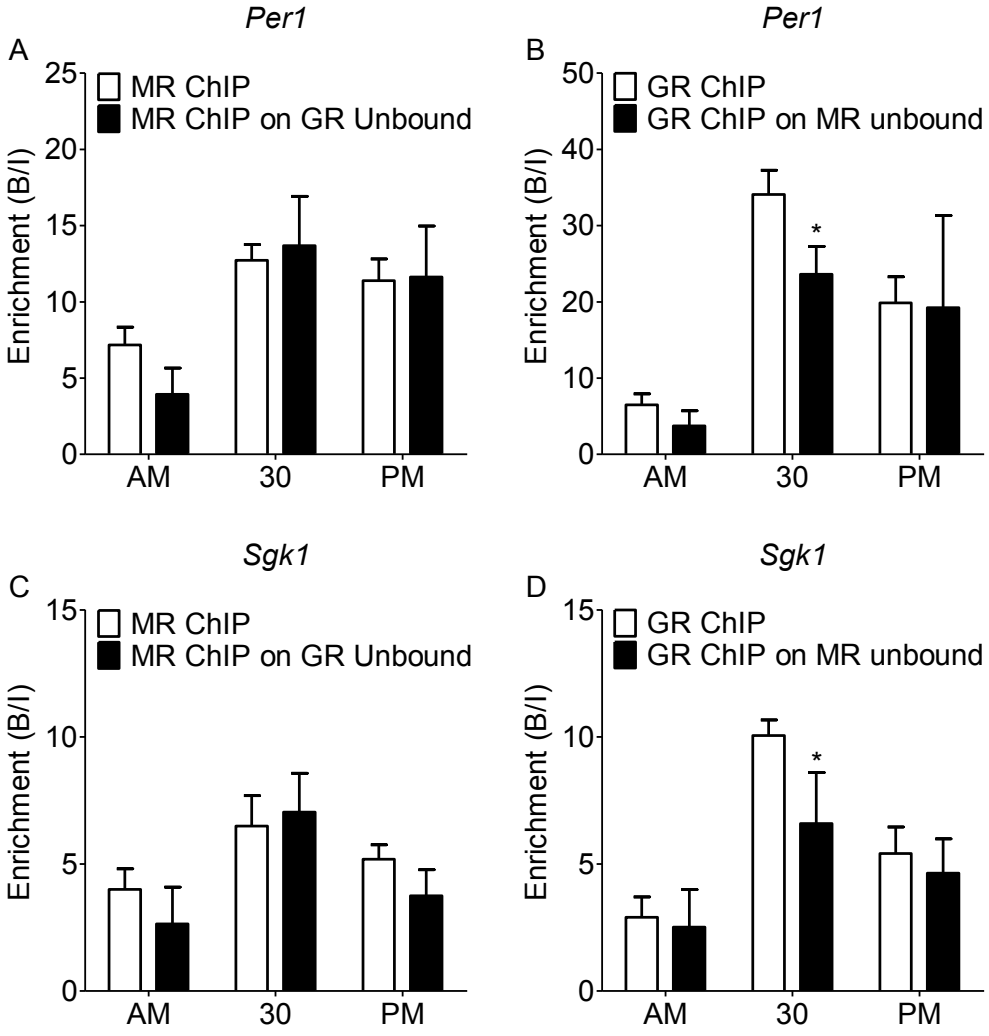
A
Per1
MR ChIP
MR ChIP on GR Unbound
Enrichment (B/I)
25
20
15
10
5
0
AM
30
PM
B
Per1
GR ChIP
GR ChIP on MR unbound
Enrichment (B/I)
50
40
30
20
10
0
*
AM
30
PM
C
Sgk1
MR ChIP
MR ChIP on GR Unbound
Enrichment (B/I)
15
10
5
0
AM
30
PM
D
Sgk1
GR ChIP
GR ChIP on MR unbound
Enrichment (B/I)
15
10
5
0
*
AM
30
PM

Figure S6

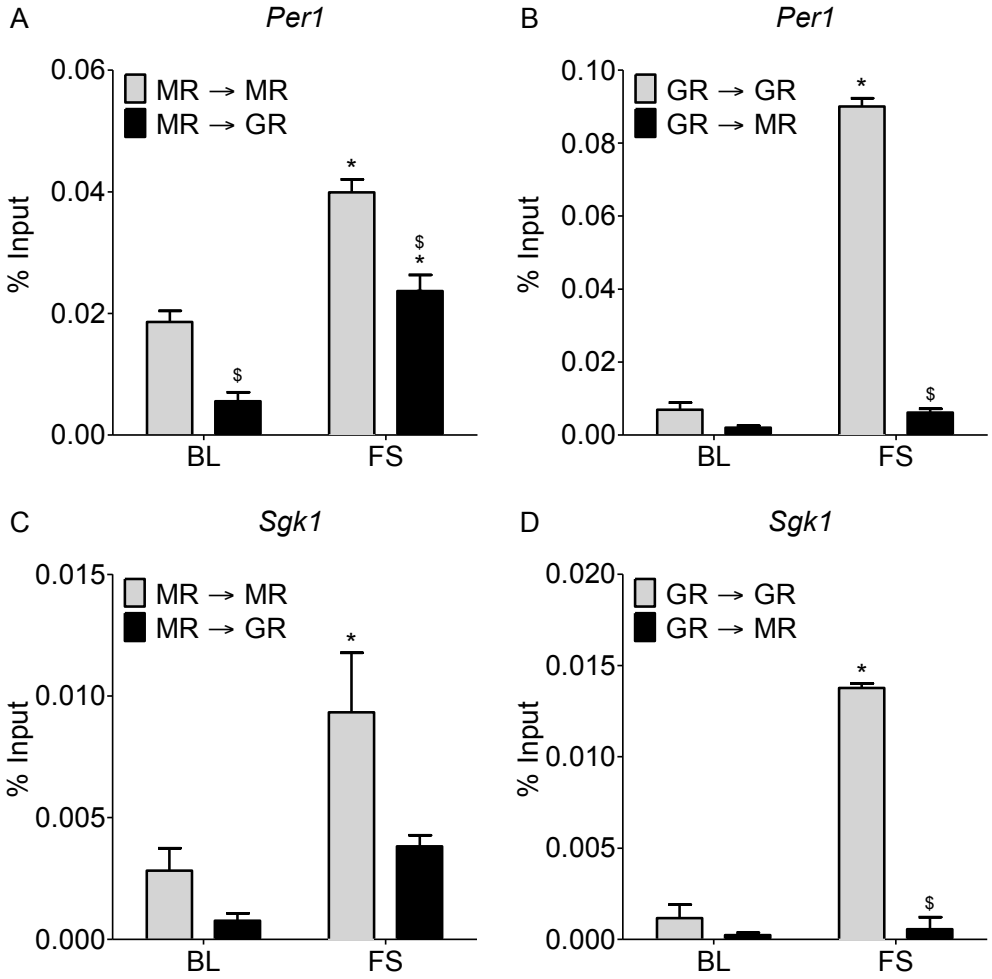
A
Per1
MR → MR
MR → GR
% Input
0.06
0.04
0.02
0.00
BL
FS
B
Per1
GR → GR
GR → MR
0.10
0.08
C
Sgk1
0.015
0.010
0.005
0.000
D
Sgk1
0.020
0.015

Figure S7

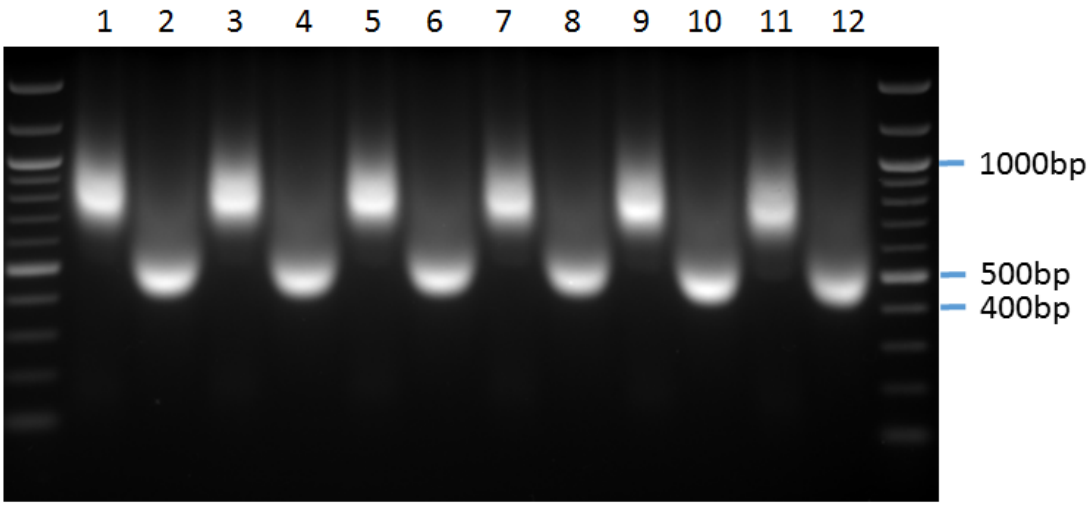

Figure S8

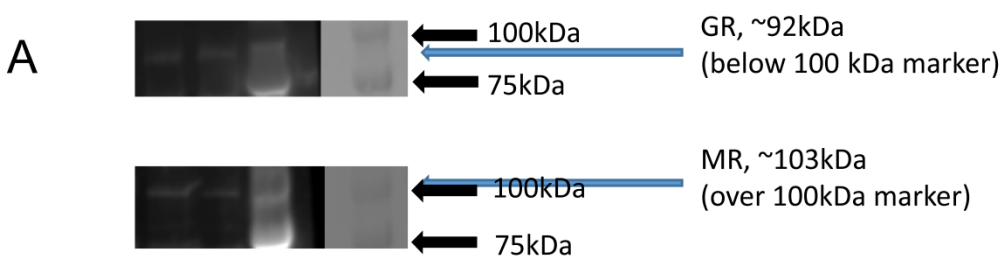
A
100kDa
75kDa
GR, ~92kDa
(below 100 kDa marker)
100kDa
75kDa
MR, ~103kDa
(over 100kDa marker)

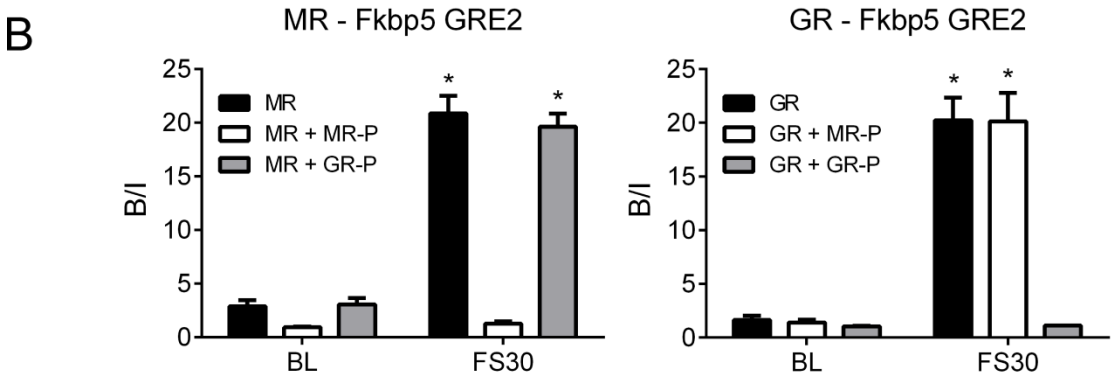
B
MR - Fkbp5 GRE2
GR - Fkbp5 GRE2
B/I
MR
MR + MR-P
MR + GR-P
GR
GR + MR-P
GR + GR-P
BL
FS30

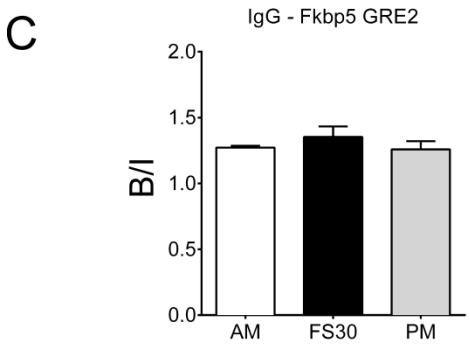
C
IgG - Fkbp5 GRE2
B/I
AM
FS30
PM

SI Table S1

Primer/Probe set	Target GRE sequence (for ChIP primers) (5' - 3')	Accession number	Forward primer sequence (5' - 3')	Reverse primer sequence (5' - 3')	Probe sequence (5' - 3')
Fkbp5 hnRNA	N/A	NC_005119.4	CCCCCCCCATTTTAATCG	TGAAGAGCACAGAACACCCTGTT	FAM - CACACCGAGTTCATGTGCCAGCCA - TAMRA
Fkbp5 mRNA	N/A	NC_005119.4	GAACCCAATGCTGAGCTTATG	ATGTACTTGCCTCCCTTGAAG	FAM - TGTCCATCTCCCAGGATTCTTTGGC - TAMRA
Per1 hnRNA	N/A	NC_005109.4	TCGCTGGCTCCTTTCACAAT	GAAAGGTTCAGGGCAGAATCAC	FAM - AACCCCCTTGTCTCCCGGCTCC - TAMRA
Per1 mRNA	N/A	NC_005109.4	CAGTGGCTGCAGCAGTGAAC	CTCCCGAAGTGCGGTCAT	FAM - AGCTCGAGCCAGGACCCAGAAAGAACT - TAMRA
Sgk1 hnRNA^	N/A	NC_005100.4	GGATGGGCCTGAACGATTT	CAATTTTCCCCAATAACCCAAA	FAM - TTGCCAACAACTCCTATGCATGCAAACAGT - TAMRA
Sgk1 mRNA	N/A	NC_005100.4	TCAGGAGCCCGAACTTATGAA	GGACCCAGGTTGATTTGTTGA	FAM - CAACCCCTCACCTCCTCCAAGTCCC - TAMRA
Hrpt1 hnRNA	N/A	NC_005120.4	TGTGCTTGCAGACCAAATACTCTTA	CGTGGATCAAGACGAGACATTG	FAM - CCACTGAGTCACCTCCCCAATGCC - TAMRA
Hrpt1 mRNA	N/A	NC_005120.4	CCTCCTCAGACCGCTTTTCC	CATAACCTGGTTCATCATCACTAATCA	FAM-CATGTCGACCCTCAGTCCCAGCG-TAMRA
Ywhaz hnRNA	N/A	NC_005106.4	GGGCACATGTGTCCGATACTG	CACCCTAGGGACAGCTTACAACA	FAM - CGCGATTGGATCCCCCGGAAT - TAMRA
Ywhaz mRNA	N/A	NC_005106.4	TGCTGCTGGTGATGACAAGAA	CATCTCCTTTTTGCTGATTTCAAA	FAM - TGGACCAGTCACAGCAAGCATACCAAGAA - TAMRA
Fkbp5 GRE1 gDNA	GGTACACGCTGTTCT	NC_005119.4	TGTGGAGGTACACGCTGTTCTTA	TGATGATTCCCCATAGCCTGTT	FAM - TGCAGGCAGAACTCCAGACTCGCA - TAMRA
Fkbp5 GRE2 gDNA	AGAACAGGGTGTTCT	NC_005119.4	CCCCCCCCATTTTAATCG	TGAAGAGCACAGAACACCCTGTT	FAM - CACACCGAGTTCATGTGCCAGCCA - TAMRA
Per1 GRE gDNA	GGAACATCCTGTTCC	NC_005109.4	CTATGCCGGTCGTGATGTCA	TGTGGCCAACAGCAAGAACTA	FAM - GCCGCTTCAGGCTGGAACATCCTGTTCCCA - TAMRA
Sgk1 GRE gDNA	AGGACAGAATGTTCT	NC_005100.4	GCCCCTGCTCCCTCTTAACTT	TCTCCGAGAACATTCTGTCCTTT	FAM - ACCTCCTCACGTGTTCTTGGCATGG - TAMRA

^ Due to complexities in the structure of the gene these primer span and exon/intron junction